Wind Energy Science

24th April 2023

Prof. Michael Muskulus
Associate Editor of the Journal,
Editorial Board,
Reviewers

RESPONSE TO THE EDITOR AND REVIEWERS

Dear Editor and Reviewers,

We would like to thank you all for your time and insightful comments about our article entitled *"A Neighborhood Search Integer Programming Approach for Wind Farm Layout Optimization"* (submission wes-2022-82), and for considering the topic and proposed method as relevant and promising.

We have made a large effort to improve the quality of the manuscript and to address all the comments and suggestions from both reviewers. The main changes are: (i) restructuring of the introduction, (ii) addition of publications from the literature and several discussions on how they compare/contribute to our work (iii) improvement of most of the figures and tables quality, (iv) reorganization of results section, (v) correction of minor aspects such as typos, writing style and other specific clarifications, and (vi) improvement of the English grammar.

Likewise, we elaborated extensively on concerns from the reviewers about, for example, the contributions from our work regarding the modelling of mixed integer linear programs, and on how the NSH performs an optimization search based on physical information from the wind turbine layouts, and not merely by just following a random search.

Below, each reviewer's comments are approached one by one.

PLEASE NOTE THAT A REVISED VERSION OF THE MANUSCRIPT WITH CHANGES FROM EACH REVIEWER MARKED WITH RED AND BLUE COLORS IS ATTACHED AT THE END OF THIS LETTER.

RESPONSE TO THE REVIEWERS

REVIEWER 1

Find below responses to each of your comments. Modifications are marked in Red:

GENERAL COMMENTS

- Comment: This work presents a new approach (NSH) to solving the wind farm layout optimization problem using a MILP approach that is made more tractable by a simplified wind

farm AEP model. The results of the model and the optimization algorithm are clearly compared to previous works and seem reasonably reproduceable. The work appears to be well-founded from a scientific perspective, is relevant to the subject matter of Wind Energy Science, and provides meaningful contributions to field. While the work is reasonably well presented, the English grammar and usage in the work present a barrier to understanding. The manuscript should be carefully, preferably professionally, edited to address these concerns so the material will be more accessible, clear, and useful to the community.

- <u>Response:</u> Thanks for appreciating the contributions presented in the article. Regarding the English grammar and usage, we have conducted a thorough review of it to improve the quality of the manuscript.

SPECIFIC COMMENTS

Abstract

- <u>Comment</u>: *Line 4-5: "deficit is aimed" I don't know what is meant by this.*

- <u>Response:</u> Thanks for pointing out this misleading statement. The word "aimed" has been replaced bv "optimized", so now this sentence should be clearer in transmitting the idea that in the power-curve-free model is optimized a measure closely related to wind speed deficit.

- <u>Comment</u>: *Line 5-6: it is unclear if the heuristic wraps the model (formulations?) or is separate. Consider clarifying.*

- <u>Response:</u> Thanks for the suggestion. As an attempt to increase clarity, this is restated as: "A special-purpose neighborhood search heuristic wraps these formulations increasing tractability and effectiveness compared to the full model that is not contained in the heuristic."

- <u>Comment</u>: *Line 8: This sentence was confusing to me, but I think I understand. Consider reworking. I think the intended meaning is that the results of the benchmark problems show that using some substitute objective rather than actual AEP can be a good approach.*

- <u>Response:</u> Thanks for the suggestion. As an attempt to increase clarity, this is restated as: "…Numerical results on a set of publicly available benchmark problems indicate that a proxy for total velocity deficit as objective is a functional approach, since high-quality solutions of annual energy production metric are obtained, when using the latter function as substitute objective…"

- <u>Comment</u>: *Line 10: "match" is probably a bit strong for the presented results, maybe say the results are competitive or something that does not indicate equality.*

- <u>Response:</u> Thanks for point this out. We agree. This sentence is restated as: "…Furthermore, the proposed heuristic is able to provide good results compared to a large set of distinctive approaches that consider the turbine positions as continuous variables."

1: Introduction

- *Comment: Line 17: I don't think I'm convinced about the importance of wind farm layout optimization by this paragraph. You state that wind energy is important politically, is presumably profitable without subsidies, and is a mature industry. The profit and maturity seem to hurt the argument for why this study is important. It sounds like things are just fine without WFLO. I'd suggest re-working this first paragraph. You could consider discussing the tight margins of wind developers and OEMs, especially offshore. You could also mention some hard values for how improved wind farm layouts could reduce the cost of energy even further. Basically, be careful to lay a clear foundation for why this work matters. You don't need to cover a lot of detail or history, but do make a clear case.*

- *Response:* Thank you for the remark. Indeed, it may read a bit as a contradiction.

We have re-phrased the paragraph focusing on why lower costs, partially achievable via optimization, are important. This content belongs to the new subsection 1.1 *Motivation and Problem Definition* after recommendation from Reviewer 2.

"…For wind energy to become the cornerstone of a successful green energy transition, further reduction in costs - partly achievable by economically optimized wind farm designs - will play an important role."

Comment: Line 24: I think you are citing Deb (2013) here for an example of a GA, but it reads like you are pointing readers to the GA that Mosetti used, only the dates don't line up (2013 vs 1994). Consider reworking this or putting the expected citation (or no citation, you already cited Mosetti which presumably has the information on the GA).

- *Response:* Thanks for the suggestion. The citation to Deb (2013) has been removed as we agree with this comment.

- *Comment: Line 26: Consider removing "and the associated numerical algorithms" because you are stating "main components". Nearly all computational methods will have "associated" algorithms. However, I'd argue that the wake combination model qualifies as a "main" component as well.*

- *Response:* Thanks for pointing out this misleading statement. The first sentence of this paragraph is changed to:
"The main components when building an optimization workflow for the WFLO problem are the wake models (deficit and superposition), the program formulation, and the associated numerical algorithms…"
We consider very important to differentiate the three aspects: wake modelling, problem formulation, and numerical algorithms. Essentially, an optimization program is set up by defining each of them according to the needs of the problem and choices of the designer. As

it is well known, there are plethora of wake models that can be used for optimization. Likewise, different problem formulations can be selected, including for example, discrete or continuous modelling, distinctive objective functions and constraints structures, among others. Lastly, it is important to emphasize that for any combination of the previous two components, several solution algorithms can be utilized, for example SLSQP, branch-and-cut, etc. This content belongs to the new subsection 1.2 *Optimization Workflow for WFLO* after recommendation from Reviewer 2.

- Comment: Line 30-34: while the wake model background may not need to be complete, the background given here is not quite correct.
1. I think Niayifar and Porte-Agel (2015) is mostly focused on the wake combination and turbulence intensity to extend the Bastankhah model to multiple turbines. In this light the citation would be better placed with the wake combination citations. Also note that there is a journal paper by the same authors from 2016 on the topic that may be a better source to cite here.
2. The Jensen cosine model was actually proposed by Jensen in 1983, so it may be good to cite that paper for the Jensen cosine model as the original source, though the Thomas et al. paper does provide some clarifications.

3. The list as given seems to show several smooth and differentiable wake models, but the combined citations seem to really only refer to two distinct wake models. I'd suggest making this a little more clear in the discussion.

4. While the sum of squares or linear combination statement is correct to my knowledge, it may be worth mentioning that the two methods have been used with local and freestream velocity conditions. This makes for four distinct proposed wake combination methods.
– Linear/freestream: Lissaman 1979
– Sum of squares/freestream: Katic et al. 1986
– Linear/local: Niayifar and Porte Agel 2015, 2016
– Sum of squares/local: Voutsinas 1990 Update: I saw you do discuss this nuance later. It may ok as is, but it did seem incomplete to me at first.

- Response: Thanks for this really good point. As the reviewer says, the wake model background may not need to be complete, but it should be improved respect to what was presented in the first version. The rest of the paragraph has been edited as

*"…*For formulating tractable frameworks, the designer needs to rely on the so-called engineering wake models. These are essentially mathematical representations which can be expressed in terms of analytical equations after significantly simplifying complex physics modelling, while still capturing to a good extent the underlying nature of the phenomenon under analysis. Scientific articles in this field have proposed and validated engineering wake models with smooth and differentiable velocity deficit shape, two examples are the Bastankhah's Gaussian (Bastankhah and Porté-Agel, 2016) or its simplified version (IEA Wind Task 37, 2019), and the Jensen cosine model

4

We consider that with these modifications the wake modelling state-of-the-art review complies with the points highlighted by the reviewer.

- Comment: Line 49: the jump from gradient-based and gradient-free algorithms to discrete algorithms was not clear and needs motivation. Consider stating the connection and purpose of the jump for those unfamiliar with the algorithms ((1) discrete methods are generally a subset of gradient-free methods, and (2) why are we talking about them here?)

- Response: We do not agree with this point, as we believe there are two modelling philosophies with respect to variable types: continuous and discrete optimization. In the subsection 1.3 *Continuous Optimization for WFLO* (please notice that after recommendations from Reviewer 2, the introduction has been split up in subsections), the continuous optimization technique is discussed. For this, both gradient-free and gradient-based algorithms have been utilized in the literature. The paragraph from lines 52 to 57 is new, where the latest work of (LoCascio et al., 2022) is discussed. In subsection 1.4 *Discrete Optimization for WFLO*, the discrete optimization technique is discussed. Within this field, both gradient-free and gradient- based algorithms have also been applied. To clarify this, the following sentence has been added:

This is an article very recently published that adopts a discrete modelling technique as well, using gradient-based algorithms to address the WFLO problem.

The objective of paragraph from lines 69 to 76 is to introduce the motivation of the focus of this manuscript, which is integer programming modelling, presenting the inhering modelling benefits of discrete optimization in this context. Subsection 1.5 *Literature Review for Integer Programming within WFLO* picks up this idea and discusses state-of-the-art in integer programming for the WFLO problem. Lastly, subsection 1.6 *Contributions* discusses the contributions of this manuscript.

Comment: Line 59-69: consider also citing https://wes.copernicus.org/articles/7/1137/2022/

- Response: Thanks for giving us notice of this very interesting work. This manuscript is cited in the paragraph from lines 52 to 57. We think that is a great addition to expand the concept of applying simpler objective functions that mitigate the complexity of optimization programs, while still being very competitive finding good solutions compared to more sophisticated models. Thereafter, this article is again cited in lines 96 to 98 to contrast it with the proxy objective function proposed in our manuscript.

Comment: Line 71: how is modeling economic metrics an advantage of the discrete model? This can and has been done in a continuous space for optimization. see https://onlinelibrary.wiley.com/doi/epdf/10.1002/we.2310

- Response: In this line it is stated "capacity to include the number of WTs as a variable and to model overall economic metrics as Net Present Value (NPV)". In the mentioned article "Optimization of turbine design in wind farms with multiple hub heights, using exact analytic gradients and structural constraints" the focus is, as the title states, on how to optimize wind farm layouts accounting for WT design. The problem assumes fixed number of WTs. It is clear that the difference lies in the fact that by a discrete modelling technique the number of WTs is considered an optimization variable. With variable number of WTs, the modelling of overall financial metrics as NPV would expose the trade-off between the number of WTs in the farm and the wake losses (AEP) vs investment costs. This is in general not possible in classic continuous optimization frameworks.

- Comment: *Line 72: (ii) can be done continuously, but it is more difficult*

- Response: In this line it is stated "…ease of modeling any shape of project area or forbidden zones, convex or non-convex…", meaning exactly what the reviewer says in this comment.

Comment: *Line 72-73: why is (iii) specific to a discrete formulation?*

- Response: In this line it is stated "…capacity to model extensive integrated models to support electrical systems optimization…". The cable layout optimization problem, which designs the electrical network to connect the WTs towards the substations, is a discrete optimization problem. It would be straight-forward to formulate a unified optimization program for the simultaneous wind farm and cable layout optimization problem, if the WFLO is modelled in a discrete way. With both problems being in the same modelling universe, it would be clear which optimization algorithms to explore. If the WFLO is modelled continuously, we cannot envisage a tractable way of tackling the unified problem.

- Comment: Line 73-74: what is the distinction between "cost functions" (iv) and "economic metrics" (i)?

- Response: An economic metric is defined in this context as the expression used to value a project from the financial perspective. NPV and IRR are examples. Cost functions refer to the mathematical representations to calculate the value of components that are required to fully compute economic metrics.

Comment: Line 74: fully continuous WFLO has been done with multiple turbine types https://www.wind-energ-sci.net/4/99/2019/wes-4-99-2019.pdf

- Response: We are aware of this. We refer to the *ease* of modelling this aspect. Therefore, the sentence is rewritten as:

"…ease of incorporating multiple WT types, among others…"

Comment: Line 76-77: consider elaborating on this idea and why discrete optimization is well suited to overcome the convexity problem

- Response: This is not the meaning of this sentence. The non-convexity nature cannot be overcome. Nevertheless, because of this feature, it is not possible to formally prove optimality. Due to this, usually different solution algorithms will converge into different final solutions. By having a diverse set of available solution algorithms, the likelihood to obtain better solutions for a given problem instance is increased.

2: Physics Modelling

Comment: Line 97-99: I'm not sure how this statement "No particular . . . " relates to the first sentence in the paragraph. Also, Thomas et al. 2022b specify some restrictions on the mathematical structure for controlling wake diameter and deficit, at least for their purpose. Specifically, the wake deficit and wake diameter must be separately controlled

- Response: Thanks for the feedback. To improve readability and connection between sentences, the statements have been rewritten like this

"The proposed MILP models and general optimization framework in this article can be easily applied to many wake deficit models. No particular properties on smoothness or differentiability are required from these models for optimization purposes. Additionally, no specific demands on mathematical structure in connection with controlling wake diameter and deficit (Thomas et al., 2022b) are stemming from the optimization programs proposed in this article…"

Comment: Line 101: from which source? there are two references

- Response: Thanks for pointing out this redundancy on the references. Reference (Dykes et al., 2015) has been deleted, because (Baker et al., 2019) is an indexed paper containing the information about wake model and benchmark results.

- Comment: Line 105: why is Thomas and Ning 2018 cited here and at line 32 for the simplified Gaussian? For the original Bastankhah wake model, I'd suggest citing Bastankhah 2016. For the simplified model, use the citation given in the following sentence (IEA Wind Task 37 2019)

- Response: Thanks for the suggestion. For the original wake model, it is cited (Bastankhah and Porté-Agel, 2016) and for the simplified model (IEA Wind Task 37, 2019), as suggested by the reviewer.

- Comment: Line 110: $d_{ij}^{\parallel}$ and $d_{ij}^{\perp}$ are not used in Eq. (1), though the coordinate frame clarifications are helpful, the symbols used seem extraneous at this point in the paper. You could possibly include these symbols as additional equations following the equation explanation of Eqs. (1) and (2) in preparation for use later in the paper.

- Response: Thanks for the suggestion. We consider that defining $d_{ij}^{\parallel}$ and $d_{ij}^{\perp}$ is useful at this point of the paper because variables $\bar{x}_\ell$, $\bar{x}_i$, $\bar{y}_\ell$ and $\bar{y}_i$ are introduced here. Trying to improve readability, this paragraph is restated as

"where u_∞ is the inflow wind speed, C_{T} is the thrust coefficient, $\bar{x}_i - \bar{x}_\ell$ is the streamwise distance from the hub generating wake ($\bar{x}_\ell$) to hub of interest ($\bar{x}_i$) along freestream (let this difference be $d_{i\ell}^{\parallel}$), $\bar{y}_i - \bar{y}_\ell$ is the span-wise distance from the hub generating wake to hub of interest perpendicular to freestream (let this difference be $d_{i\ell}^{\perp}$), σ_{y} is the standard deviation of the wake deficit, k_{y} is a variable based on a turbulence intensity, and D is the WT diameter."

- Comment: Line 115: consider removing one of these duplicate mathematical statements.

- Response: Thanks for noticing this typo. It has been fixed.

- Comment: Line 125-130: The references used to arrive at Eqs. (6) and (7) were given in the introduction, but I think it would be helpful to provide them again here.

- Response: Thanks again for this recommendation. The references have been added above Eq. (3), Eq. (4), Eq. (6), and Eq. (7).

Comment: Line 133: why is the power curve non-differentiable specifically at rated wind speed? The definition provided in this manuscript is non-differentiable at the rated power, but the continuity of the power curve is just dependent on the power curve definition, so this statement is not correct in general.

- Response: We have modified this subsection as follows to improve the technical rigor

"Suitable power curves are required for computing AEP. Often, power curves are not perfectly suitable for optimization, due to the usual non-differentiability in several points throughout the function. Generally, a power curve is zero below cut-in wind speed, zero above the cut-out wind speed, and constant between the rated wind speed and the cut-out wind speed. In this particular study, between the cut-in and rated wind speeds the curve is assumed to be smooth, convex and monotonically increasing. The simplified power curve for a generic turbine as a function of wind speed u is modelled through…"

"…where p^{rated} is the nominal power at (and above) rated wind speed u^{rated}. The other turbine characteristics are the cut-in wind speed u^{cut-in}, and the cut-out wind speed $u^{cut-out}$. In this definition, the WT power curve is not differentiable at u^{cut-in}, u^{rated}, $u^{cut-out}$, since in these points the left and right hand side derivatives are different. Be aware that the optimization programs proposed in this manuscript are not dependent on WT power curve differentiability." The non-differentiability discussed here is naturally dependent on the power curve definition. However, the one presented aligns with the usual function recurrently implemented in the literature.

3: Optimization Models

- Comment: Eqs. (12) to (14) The presentation here is difficult to follow. Perhaps consider breaking them up into more equations with more explanation and grouping by interval (1, 2, a+1, m+1, m+2).

– the statement "for a = 1,. . . ,m" should be applied to each numbered equation it applies to individually.

– I'm not sure how the delta u is supposed to be applied in Eq. (13). Re-working the presentation of these equations should help.

– are "a" and "l" being used for the same thing here? If so, correct. If not, please clarify.

– There may be a better way to present the interval values, the above are just my ideas at the moment.

- Response: Thanks for this observation. This part has been reworked as presented in the next page.

We hope that this improves the readability of this part. The statement "for a = 1,. . . ,m" has been applied individually in Eq. (14) and in Eq. (15), meaning each of the subintervals sampled within the cubic subdomain of the whole WT power curve domain. The value of Δu has been explicitly declared in the paragraph preceding the equations. Lastly, a and l represents different things. The variable l is for any interval in the whole domain of the curve, while a is for an interval located in the cubic domain.

"

cut-out speed. Each isometric interval within the cubic domain of length $\Delta u = (u^{\text{rated}} - u^{\text{cut-in}})/m$, is approximated with a constant power value, see Fig. 1.

An interval l of the whole domain is characterized by three parameters u_{s}^l, u_{m}^l, and u_{h}^l with the next properties

$$u_{\text{s}}^1 = -u^{\text{ini}}, u_{\text{h}}^1 = u^{\text{cut-in}}, u_{\text{s}}^{m+2} = u^{\text{rated}}, u_{\text{h}}^{m+2} = u^{\text{cut-out}} \tag{12}$$

$$u_{\text{s}}^2 = u^{\text{cut-in}}, u_{\text{h}}^{m+1} = u^{\text{rated}} \tag{13}$$

$$u_{\text{s}}^{a+1} = u^{\text{cut-in}} + (a-1)\Delta u \text{ for } a = 1,\ldots,m \tag{14}$$

$$u_{\text{h}}^{a+1} = u^{\text{cut-in}} + a\Delta u \text{ for } a = 1,\ldots,m \tag{15}$$

$$u_{\text{m}}^l = 0.5(u_{\text{s}}^l + u_{\text{h}}^l) \tag{16}$$

"

Equation (12) defines the lower and upper limits for the extreme intervals $l = 1$ and $l = m + 2$, Eq. (13) formalizes the lower and upper limits for the first interval in the cubic part, $a = 1$, and the last one $a = m$, respectively. Equation (14) expresses the lower limits for intervals in

9

the cubic part ($a = 1, \ldots, m$), while Eq. (15) does it for the upper limits. Equation (16) presents how to determine the extracted wind speed associated to the interval l of the whole domain, which is the average value of u_s^l and u_h^l."

- *Comment: Eq. (16a): xi, eta, and u are specified as design variables, but I think eta and u are state variables dependent on xi, so it seems that xi represents all design variables. I've only seen design variables represented in the sub-scripted variables under the "maximize" in the optimization equation.*

- *Response*: The reviewer is right about the fact that eta and u are state variables fully dependent on xi. However, we do not agree with the observation that the subscripted variables under "maximize" should only present fully independent variables. For completeness, we chose to present all variables required in an optimization program, regardless of relation of dependence between them. On the other hand, the article explains clearly the difference between binary variables \xi and the state ones eta, u, and tau.

- *Comment: Section 3.2: this approach appears similar to the FLOWERS model found in https://wes.copernicus.org/articles/7/1137/2022/wes-7-1137-2022.pdf. I'd suggest contrasting the method in the submitted manuscript to the FLOWERS model, perhaps in the introduction, but referring back to it again here.*

- *Response*: This manuscript is cited in the paragraph from lines 52 to 57. Thereafter, this article is again cited in lines 96 to 98 to contrast it with the proxy objective function proposed in our manuscript. Finally, this article is referred back in this section in lines 269 to 271 as "This proxy objective function is very useful for formulating the program in the MILP category. While the work in (LoCascio et al., 2022) focuses on a different formulation (likely more accurate analytically than the one presented here) that is non-linear but gradient friendly, hence useful for continuous gradient-based optimization."

- *Comment: Line 204: I need a little clarification regarding which "outlook" the IEA 37 studies follow.*

- *Response*: We have rewritten this sentence to improve readability as follows
"Albeit the formulation of Sect. 3.1 represents to a very large extent the physics ruling the problem, it has a considerable number of variables and constraints that may hinder the capacity to tackle larger problems. The model presented in this section neglects power curve and AEP calculation and aims at simplifying the power-curve-based version.

The model deploys a strategy to account for the combination of Eq. (3) and Eq. (7) to calculate velocities, since the case studies from the IEA Wind Task 37 follow this methodology for AEP computation. It would be possible though to consider the linear superposition model if necessary. However, the power-curve-free model does not support the application of Eq. (4)."

We mean that that approach is considered in this section for AEP computation, following the methodology implemented in the IEA37 Wind Task.

- *Comment: Line 211: please provide justification for dropping the square roots. Why is the model expected to be correct if the square root is simply "dropped"?*

- _Response_: We acknowledge that by simply dropping the square roots the model is not "correct", but expect that the resultant expression, incorporated in the MILP model, is "*good enough*". Line 244 in the new version of the manuscript is added:

"…the arguments of the square roots in Eq. (19) define a function closely related to the full root-squared expression…"

To have a better idea about this premise, please see the below plot
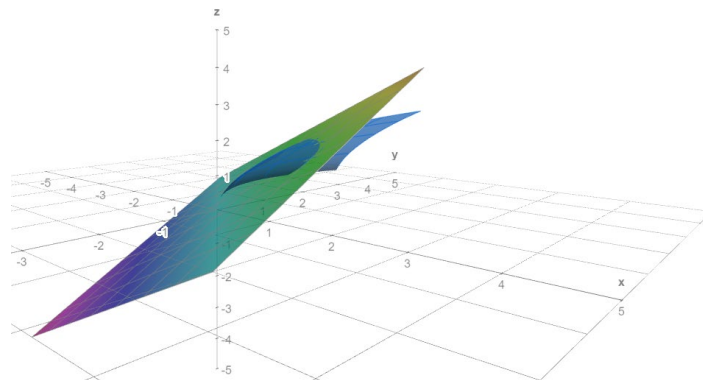
The plane plot is of the function $z = x + y$ and the other one is for $z = \sqrt{x} + \sqrt{y}$. Note how these two functions follow relatively close to each other for non-negative values of x and y. A similar behavior is expected between the original root-squared expression and the other one that ignores them.

Practical evidence of the accuracy of this simplification is presented in Table 1.

- _Comment:_ Eq. 20: how did you get to b_{i,l} + b_{l,i} and the l>i? I don't see offhand how those terms come from combining eqs. 18 and 19 as stated.

- _Response_: As variable $z_{i\ell}$ represents that both WTs in i and j are selected, then when it is zero, the mutual influence given by summing up both $b_{i\ell}$ and $b_{\ell i}$ must also be zero. By defining the second sum with $\ell > i$, the number of variables is halved after this symmetric property.

4: Neighborhood Search Heuristic

- _Comment:_ Alg. 1, Line 13: check spacing

- _Response_: Thanks for noticing this typo. It has been fixed.

- _Comment:_ Line 263-264: what is meant by "stopped until"?

- _Response_: Thanks for noticing this misleading statement. It has been restated as "…The complete model is sent to the MILP solver with ξ as warm-starter, stopped when reaches either optimality or the assigned maximum computing time T…"

- _Comment:_ The NSH algorithm seems similar to the one developed by Paul Malisani and presented in "A Comparison of Eight Optimization Methods Applied to a Wind Farm La out

Optimization Problem" by Thomas et al. (https://wes.copernicus.org/preprints/wes-2022-90/). Consider comparing and contrasting the approaches.

- *Response*: Thanks for giving us notice of this very interesting work. We have added this work in the introduction (paragraph from lines 99 to 109) as

"The second main contribution is the proposition of a new special purpose neighborhood search heuristics in order to speed up the generation of high-quality solutions. This heuristic, wrapping both formulations, has a twofold functionality; first to increase tractability, and second to redirect the optimization search in terms of a specified objective function with higher fidelity. Similar neighborhood search methods have been proposed in the literature, as the Discrete exploration-based optimization (DEBO) (Thomas et al., 2022c), which is a two-steps process composed by a greedy initialization and a local search block. While the method proposed in this manuscript shares most of the advantages of the mentioned approach (no gradients required, can handle unconnected and non-convex boundary constraints, and so on), it actually goes beyond the DEBO algorithm as among others, i) significantly less AEP function evaluations are required, and ii) it is based on well-establish integer programming theory, relying in efficient implementations of the branch-and-cut algorithm. The main numerical results indicate good computational performances for a set of publicly available benchmark case studies compared to state-of-the-art gradient-free and gradient-based approaches (Baker et al., 2019)."

This article is referred back in this section in paragraph from lines 305 to 307 as

"… One of the advantages of the NSH compared to the DEBO algorithm (Thomas et al., 2022c) is the reduced number of AEP evaluations. In an iteration κ, only |S| evaluations are required. Likewise, many of the other expensive calculations are done in a preprocessing stage…"

"…Another difference between the NSH and the DEBO is that the latter only changes the position of a single WT in a given iteration, while the former considers simultaneous modifications of several WT positions." (lines 312 to 314).

5: Computational Experiments

- *Comment:* Line 286: why these parameter values?

- *Response*: In the line 320 has been added the reference for benchmarking
"The main parameters of the wake model in Sect. 2.1 are fixed to CT = 8/9 and ky = 0.0324555, according to (Baker et al., 2019)"

- *Comment:* Line 299: it would be nice to see all non-default parameters (the introduction "for example" seems to indicate that only some of the non-default parameters are given). Consider putting in a table with the non-default parameter values.

- Response: This paragraph has been modified to
"…The selected MILP solver is the commercial branch-and-cut algorithm implemented in IBM ILOG CPLEX Optimization Studio V20.1 (IBM, 2022). Apart from the number of threads and time limit settings, a few other parameters are also set to different values compared to the

default choices as well. One is the parameter returning high-quality feasible solutions early in the process, for which, the (CPX_MIPEMPHASIS_HEURISTIC) is activated. The intention is to generate more feasible layouts which is important for the neighborhood search algorithm. Additionally, strong branching is used for variable selection given the large size of the models (CPX_VARSEL_STRONG is selected). The intention is to reduce the size of the search tree and thus the memory requirements compared to default settings."

Since these are the only settings that have been changed from default values, we choose not to add a table for this purpose to avoid enlarging the paper's length.

- *Comment:* *Line 305-316: was this sampling method compared to any other methods?*

- Response: Not being the objective of the manuscript to evaluate different sampling methods, this has not been exhaustively investigate. One of the experiments not included in the article was to use a Delaunay-triangulation-based sampling of the 1300 m radius circumference. Using the same algorithm parameters, the presented method in the manuscript consistently improved the Delaunay one. Because more experiments should be done to elaborate a comprehensive comparison, no discussion is presented in this matter. This could be an interesting support work to perform in the short-term future.

- *Comment: Line 334: how do we know it is "still strong enough"? What was the bar?*

- Response: Thanks for the feedback. We agree with the fact that this expression may sound as comparative to a well-defined standard. Instead, this sentence has been modified to
"..In spite of this deterioration, the linear correlation is still considered quite strong.."
Although the range of correlation coefficient values and the corresponding levels of correlation vary depending on the application context, a correlation in the interval [-1 to -0.80] is usually deemed as 'Very Strong Negative', and between [-0.79 to -0.60] as 'Strong Negative'. See for example reference https://www.ccsenet.org/journal/index.php/cis/article/view/59661.
Since we do not aim to provide a formal definition of this aspect, adding the word "considered" should highlight the subjective meaning intended.

- *Comment: Line 346: which model is "exact"? All the models presented in this paper appear to be approximations.*

- Response: This comment refers to the general finding of the article that focusing on total wind speed minimization (or its use to calculate an approximated AEP function) is a promising research line for the WFLO problem.

- *Comment: Line 349: Perhaps the "deterioration" is partly due to "dropping" the square root?*

- Response: This is true and it is actually discussed in the lines 383 to 390.

- *Comment: Line 349: "this" is unclear, state meaning explicitly*

- Response: It has been replaced "this" by "…Case III…".

- *Comment: Table 1, Fig. 4: beautiful use and presentation of correlation. Nice work!*

- Response: Thanks!

- Comment: Line 363: It would be helpful to provide more information about the tuning process.

- Response: Since we consider that there is not an optimal way of tuning these parameters, no extensive discussions are deployed. These settings were obtained after few trial and error. Some general annotations are given in the following lines about the reasoning behind the presented values of C, T, and V.

- Comment: Line 363: My understanding of C, T, and V was incomplete and I had to go back and re-read previous sections and this sections to get straitened out. I'd suggest adding more explanation of these inputs when you introduce the algorithm.

- Response: Done. This is carried out by
"..The main inputs are C = {467, 590, 1014} (set of candidate locations), T = {1, 1.5, 2} h (set of max computing times for each candidate location), V = {2, 4, 6, 16} (set of neighborhood search sizes). See Sect. 4..."

- Comment: Fig. 5: – are the times shown clock time or CPU time? – while run time is helpful, it can vary drastically depending on implementation, language, system, etc. You may want to consider also including a count of total calls to your objective function.

- Response: It is indeed clock time and it has been clarified in Line 392.

To our knowledge, function evaluation metric is usually used to assess metaheuristic algorithm's performance as they depend upon the number of generations and the size of the population, so it is an indication of the efficiency of the algorithm, considering a given computing time to assess the fitness function once. Some gradient-based solver also provide this metric. However, the proposed method uses an exact formulation and calls an external state-of-the-art solver using branch-and-cut method to get high-quality solutions. We see that the vast majority of works in the operations research field using solvers as CPLEX report clock time as normal practice. See for example https://link.springer.com/article/10.1007/s10732-015-9295-0#:~:text=Relax%2Dand%2Dfix%20(RF,in%20their%20sophisticated%20lot%2Dsizing, or https://www.sciencedirect.com/science/article/pii/S2211692317300188.
This is usually the case because branch-and-cut black-box solvers do not easily provide this information.

- Comment: Fig. 6, 8: – Are your wind turbine markers to scale? – This figure is missing axis labels – This figure is missing units for the tick labels

- Response: Markers are not to scale. Figures 3, 6, and 8 have been edited so axis labels and units for ticks are added.

- Comment: 5.3: the baseline of the percentages given is unclear. Is each percentage given using the last step level as the baseline or the original "incumbant" value?

- Response: The baseline is the last step commented. In line 449-450 has been added the sentence

"…As for Case I, improvement percentages are calculated using the last commented step as the baseline…"

- *Comment*: *Fig. 7: perhaps I missed where this was stated, but are all the AEP values here calculated using the full model for comparison? If not, I think they should be.*

- Response: Correct. This is stated in line 320-326.

- *Comment*: *Eq. 23: The equation in your reference is general, but you provide a specific version here. It would be helpful to introduce the general form of your equation from your reference and then fill in the specifics. You may also want to use a more concrete reference here than Investopedia. There are many for this material.*

- Response: From lines 502 to 507, the following description has been added

"…. The general form of the NPV equation (Cogency, 2014) is defined by the sum of the present value of cash flows (Discounted Cash Flow, DCF) of a project under analysis. In Eq. (25), the first sum is a negative cash flow representing purchase of the WTs at the construction stage of the project, while the next term represents positive cash flows coming from trading the electricity in the market. Because of the additive nature of the NPV metric and since the focus is on evaluating investment vs revenues, by maximizing Eq. (25), a fully comprehensive NPV metric is equivalently improved."

- *Comment*: *Line 474: The last sentence here needs more explanation.*

- Response: By expanding the previous paragraph and with the following sentence, we consider that the explanation has been improved

"When the number of turbines is fixed to 10, the NPV evolution (green line in Fig. 11b) is driven by the AEP (green line in Fig. 11a). Both curves are monotonically increasing, reaching a final value of NPV of = 456.40 mEUR. The same behaviour is visible for n_T = 50, although the final NPV is greater (683.53 mEUR), see blue line Figure 11b. In the second study, the positive difference in DCF from the revenues surpasses the associated extra investment costs from the additional 40 wind turbines considered. The significant increase in the number of WTs doubles the computing time, due to the large increase in the number of variables, selecting 50 WTs entails significantly more possible combinations of valid solutions."

- *Comment*: *Line 476: I'm not sure what you mean, but if it is the main question then I should. Can you be more specific and/or clarify?*

- Response: The sentence is restated as

"…An interesting question is whether there is a larger NPV in between the bounds of WT number…."

- *Comment*: *Fig. 11-13 would probably be more clear if combined and corresponding lines were plotted on the same axes*

- Response: Thanks for the advice. The recommendation has been followed and the descriptive texts have correspondingly been adapted.

TECHNICAL CORRECTIONS

General

- *Comment*: *There are many grammar and usage errors throughout. The manuscript should be carefully edited to address these concerns so the material will be more accessible and useful to the community. I have noted a few of these below.*

- Response: We have conducted a thorough review of it to improve the quality of the manuscript.

1: Introduction

- *Comment*: *Line 13: "Subsidy-free . . . " check grammar*

- Response: Done.

- *Comment*: *Line 19: Because you give a list of parts here (rather than just one primary thing), "consists of" may be more appropriate.*

- Response: Done. Thanks for the advice.

2: Physics Modelling

- *Comment*: *Line 132-133: comma after AEP*

- Response: Done. Thanks for the advice.

- *Comment*: *Eq. (8): this piece-wise equation contains multiple definitions for some cross-over points. Check the usage of "<" vs "<="*

- Response: Thanks for noticing this typo. We had seen it in advance, and it has been corrected.

3: Optimization Models

- *Comment: Line 145: check commas to ensure clarity*

- Response: Done. Thanks for the advice.

- *Comment: Line 200-203: check grammar and usage to ensure clarity*

- Response: Done. See full paragraph.

…Albeit the formulation of Sect. 3.1 represents to a very large extent the physics ruling the problem, it has a considerable number of variables and constraints that may hinder the capacity to tackle larger problems. The model presented in this section neglects power curve and AEP calculation and aims at simplifying the power-curve-based version."

- Comment: Line 205: does "this" refer to the linear superposition model or the powercurve free model? In general, try to avoid "this" where there is any possibility of misinterpretation.

- Response: Thanks for the advice. Corrected as

"…However, the power-curve-free model does not support the application of Eq. (4)…"

4: Neighborhood Search Heuristic

- Comment: Line 243: observation should be singular

- Response: Thanks for noticing this typo. It has been corrected.

5: Computational Experiments

- Comment: Fig. 4: This figure is a little busy, consider giving the figures a little more space by removing all unnecessary elements and adding some buffer space between sub-figures and figure elements. I really like this figure overall though.

- Response: Thanks for the advice. The AEP units in this figure has been changed to GWh and a buffer space between the top sub-figures has been added as well.

- Comment: Line 276: radii

- Response: Thanks for noticing this typo. It has been corrected.

- Comment: Line 412: I suggest avoiding starting a paragraph with "As shown in Fig. x" because we don't even know what the subject of the paragraph is yet. The "as shown. . . " should fit well at the end of the sentence.

- Response: Thanks for the advice. It has been corrected and checked throughout the manuscript.

- Comment: Figures in general: – The units given sometimes lead to very large numbers that clutter the figure and impede interpretation. I'd suggest using units that reduce the number of digits required in the tick labels (i.e. GWh instead of MWh, and hours or days instead of seconds)

- Response: For Figure 4 and Figure 11 this comment is particularly useful and it has been applied. For Figures 5, 7, and 9 the ordinate units has been changed to GWh. The abscissa units (s) has been kept according to the needs of the descriptive text.

REVIEWER 2

Find below responses to each of your comments. Modifications are marked in Blue:

REVIEWER SUMMARY

- Comment: The authors consider the wind farm layout optimization problem. Their contribution are a pair of discrete optimization algorithms. These consist of an inner and outer optimizer. Starting from an initial proposal solution (feasible layout) The inner optimizer generates a set of candidate solutions (feasible layouts; 'pool') using a MILP solver applied to a linearization— thus approximation—of the classical AEP objective. (The authors propose two such linearizations, hence the pair of algorithms.) The outer 'NSH' optimizer calculates the exact, non-approximated AEP values for the candidate solutions and selects the best one as the proposal for the next MILP run (or the final solution, upon algorithm termination) and determines the parameters for the next MILP run.

The authors motivate their work by pointing out the advantages of discrete optimization algorithms when moving beyond classical AEP calculations to objectives such as NPV which also take into account costs, such as those of turbines, their installation, and the cabling. In support of the linearization of the objective—which is needed to use well-developed, capable MILP solvers—they present an analysis of the correlation between the AEP and the simplest linearized objective based on their application to a set of random layouts. To demonstrate their algorithms, they apply them to the IEA Wind Task 37 Case Study 1, which consists of three layout optimization problems with a disc-shaped site with different sizes and (fixed) turbine numbers. Furthermore, they also modify the Case Study problem, to show that one of the two algorithms can optimize NPV by varying both turbine locations and counts.

GENERAL EVALUATION AND KEY CRITICAL FEEDBACK POINTS

- Comment: I was able to follow the exposition without much rereading, so generally I consider the paper to be written at good levels of abstraction and detail and well-structured. The quality of the writing is decent: while the meaning is generally clear, the reader is distracted by some strange formulations, likely due to the authors not being native speakers of English. This can be fixed by having a (near) native speaker going over the paper just focusing and providing feedback on English usage (some pointers will be given in the detailed feedback). The paper's visuals and tables are generally OK, but can be improved in some detailed aspects (pointers will be provided in the detailed feedback). The mathematics as well is generally fine, but the notation can be introduced with a bit more care to support understanding and avoid confusion (pointers will be provided in the detailed feedback).

I agree with the paper's motivation for developing a discrete wind farm layout optimization algorithm, but did not find the argumentation sufficiently concrete or precise. Make it more explicit what and how is difficult to do with continuous optimization algorithms and easy with discrete ones. A weakness of the paper is that it only demonstrates the advantages of discrete optimization by looking at one optimization problem that goes beyond the basic AEP optimization over a convex site only by making the turbine count a design variable. Furthermore, the choice of benchmark used, IEA Wind Task 37 Case Study 1 is not anymore

state-of-the art; something like Case Study 4, with a more realistic site complexity and more realistic wind resource modeling would be a more appropriate comparison point (cf. the paper on this Case Study currently also under review: https://wes.copernicus.org/preprints/wes-2022-90/ [disclosure: I contributed to this work]). Ideally, such a more realistic benchmark would be included, but this may be too much to ask, so I would leave such decision to the editor.

The correlation analysis to support the use of one of the proposed linearized objectives is useful to show that it makes sense to try out its use, as indeed there is sufficiently strong correlation within a random set of layouts. However, I find correlation for a random set of layouts insufficient justification for concluding that its use is warranted. Namely, during a MILP run, the layouts will very much not be random and will be very similar to each other, so it would need to be shown that for such sets of layouts there also is correlation. This can be done by comparing the rankings produced by the linearized objective and the AEP for all of the solutions in a pool, for each of the pools. It is my opinion that such an analysis should be added, because based on the current information, it could still be the case that the inner MILP optimization's added value is limited, as there is mostly a random search happening. (It the plots 5, 7 and 9, the flat parts suggest such behavior and the sloped ones not.)

Mathematical programming techniques (linear, quadratic, with and without integer variables) have been used in the context of wind farm layout optimization by many researchers. Also, linearization of objectives to be able to use MILP solvers is a common technique. The paper gives a decent selection of references about this. It can make the connection to the existing literature more explicit, however. Namely, what is it precisely that is new in this work, which was not done yet (in this context)? Specifically, I feel that the work of Turner et al. (2014) should get more credit and mention in your discussion, as they present a linearization that is very close to your power curve-free approach (compare your Eqs. 17-19 with their Eqs. 3, 7, 9 and your discussion on page 9 line 219-220 with their Eq. 10). As far as I can see, your contribution here is applying a big-M trick, which reduces the problem's complexity.

Similarly, a bit more can be said about search heuristics both in wind farm layout optimization and other application domains to contextualize your NSH algorithm. (Such search algorithms are quite common, also in nested optimization algorithms.) Here, I am not aware of as close a counterpart as with Turner et al. (2014) for the MILP part, but some example references are http://dx.doi.org/10.1016/j.renene.2015.01.005 (the most important one, according to me), http://dx.doi.org/10.1016/j.renene.2012.07.021, and methods in https://wes.copernicus.org/preprints/wes-2022-90/ such as ADREMOG [disclosure: I was involved in the creation of this algorithm].

The discussion of the application of the presented algorithms to IEA Wind Task 37 Case Study 1 presents information about their practical computational efficiency. The computational time needed shows the approach to be very computationally demanding (order of 10 h, 20 h, 40 h, respectively for the sites with 16, 36, and 64 turbines), which impedes its use and therefore decreases its practical relevance. Certainly the variant using a stepwise-constant approximation to the power curve is problematic in this regard, as on very performant hardware it takes 36 hours on the smallest case to perform noticably worse than the power curve-free variant (using about 15 h on quite standard workstation laptop hardware). In the IEA Wind Task Case Studies, there was a wide range of computational efficiencies in the algorithms presented, but there were multiple competitive ones that were substantially more efficient than

the approaches presented here. As an example, the approach that I contributed to the Case Studies is the one based on pseudo gradients (cf. https://wes.copernicus.org/articles/6/815/2021/). The authors mention the results of this approach with their own by stating that they can achieve similar results in 2 and 3 hours (16 and 36 turbine cases) and that this is 'way faster' than for 'these kind of algorithms'. I re-ran the case studies with the (current, more flexible, but more involved) version of the pseudo-gradient algorithm and obtained the following results (on a laptop that is roughly 2-3 times as fast as the one used by the authors), to be compared to the values in Table 1:

- *16-turbine case: 4 seconds to obtain 403 GW layout; 1 minute to obtain 409 GW layout*

- *36-turbine case: 7 seconds to obtain 833 GW layout; 2 minutes to obtain 844 GW layout*

- *64-turbine case: 45 seconds to obtain 1466 GW layout; 2 minutes to obtain 1480 GW layout*

While the pseudo-gradient algorithm was created for supporting a more interactive form of wind farm design and therefore is not able to obtain the highest AEP values seen, these computation times should help recalibrate the author's view of what is typical in state-of-the-art wind farm layout optimization. Understandably, I feel it is required that the authors update their mention of typical times of approaches they compare to.

- Response: Thanks for your feedback. We respond to each of the comments contained in this section as follows:

- English usage: We have thoroughly checked the English grammar throughout the manuscript to improve its quality.
- Paper's motivation for developing a discrete wind farm layout optimization algorithm: We have modified the whole introduction section. This point should be clearer now. With discreet optimization, when the problem consists of complexly shaped wind farm areas, as a set defined by disconnected non-convex polygons, simply generating a set of candidate locations within these areas would suffice to satisfy the domain constraint. While we have no direct experience in applying continuous gradient-based algorithms for this case, the available literature indicates increased complexity, since functions based on minimum distance to the set of vertices of a polygon, and customized functions to evaluate if a point is inside or not of that shape, must be incorporated. The full effect of using these functions in the context of gradient-based optimization does not seem to be known. However, one expects that due to the non-differentiability of the functions throughout the whole domain, the performance of numerical algorithms will be impacted.
  Other advantages of discrete optimization approach are the ability to easily consider a variable number of installed wind turbines, or more interestingly for us, capacity for unified optimization with electrical systems (cable layout). To the best of our knowledge, no implementations using continuous optimization are available for the unified problem.
  The Case IV in paper *https://wes.copernicus.org/preprints/wes-2022-90/* was not available to us at the development stage of the methods and during the preparation of the first version of the manuscript. As the reviewer argues, for the presented cases (Cases I, II, and III from the IEA first benchmark), some of the benchmark algorithms (gradient-based or pseudo-gradients) are computationally faster than our proposed

methods. Nevertheless, the main aim of the manuscript is to provide a proof of concept of the methods. While evidently slower, the comparison is aimed at showing that the results obtained by the proposed methods are in the same quality range as the benchmark.

In the paper *https://wes.copernicus.org/preprints/wes-2022-90/* the best results are obtained after applying the DEBO algorithm, which follows a discretized modelling technique as well. This should be understood as an advantage of our proposed methods, showing the promising potential of the method for instantiations of the WFLO problem beyond classic definition.

- <u>Correlation proxy total velocity deficit vs AEP:</u> Based on the reviewer's suggestion, we have extended the plot from Fig. 4c by including all solutions from each solution pool when executing the NSH using model (23) (total wind speed deficit proxy) for Cases I, II, and III. The results for Case I clearly show that the layouts are not random and are similar to each other in a most of the iterations within the NSH. See Fig. A. While it is true that in a solution pool in a given iteration the correlation can be worse (for example, in the box of [0.30 m/s-0.39 m/s,407 GWh-414 GWh], see Fig. B), this negative effect is corrected by the NSH (line 13 in Algorithm 1 in the manuscript), by choosing as new incumbent for next iteration the best solution in terms of AEP. See Fig. C. We see that the frequency of occurrence of low correlation within the solution pool in a specific NSH iteration is limited.
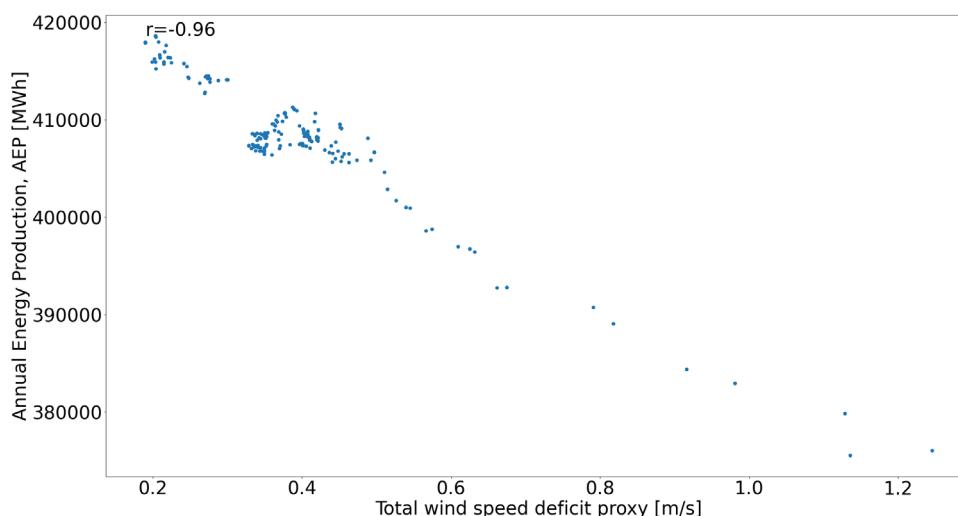
Figure A. Correlation plot AEP vs Linear objective for all solutions in all pools for Case I (total number of feasible points of 229)
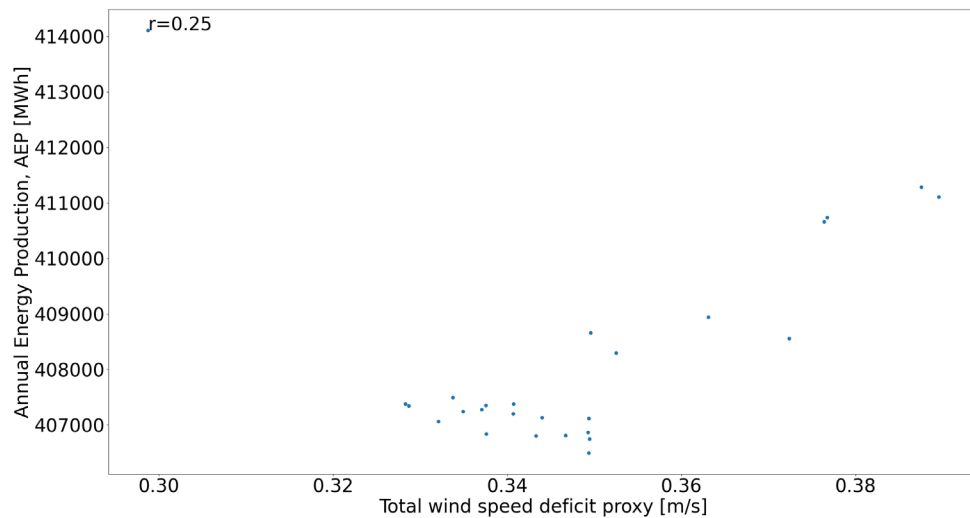
Figure B. Correlation plot AEP vs Linear objective for solutions in a single pool for Case I
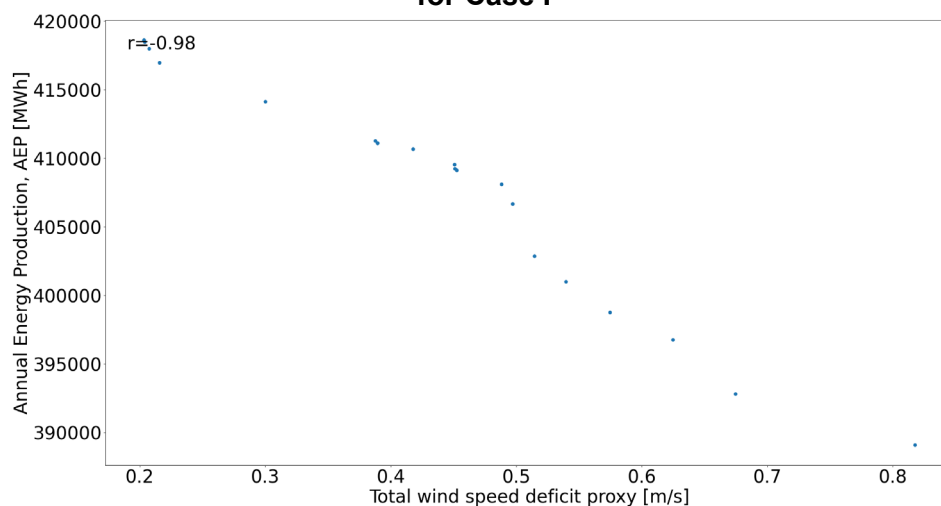
Figure C. Correlation plot AEP vs Linear objective after NSH correction for Case I

As presented in Table I, we see that the correlations deteriorate for the larger case studies. This is also the situation in the solution pool analysis, as illustrated in Fig. D to Fig. G for the 36 and 64 WTs cases. The solution pools with a low correlation are marked with red circles in Fig. D and Fig. F. Correspondingly, Fig. E and Fig. G show how the NSH helps in improving the correlation metrics from the point of view of incumbent generation, by recentering the optimization search around a new point in an iteration $\kappa + 1$, only if it improves the best-known solution at κ. The total number of feasible points in each case after summing up in all pools is relatively low: Case I - 229 valid WT layouts generated throughout the entire optimization search (and 412 and 714, respectively, for the next two cases). With a random search, the number of valid

WT layouts would, intuitively, be significantly larger.
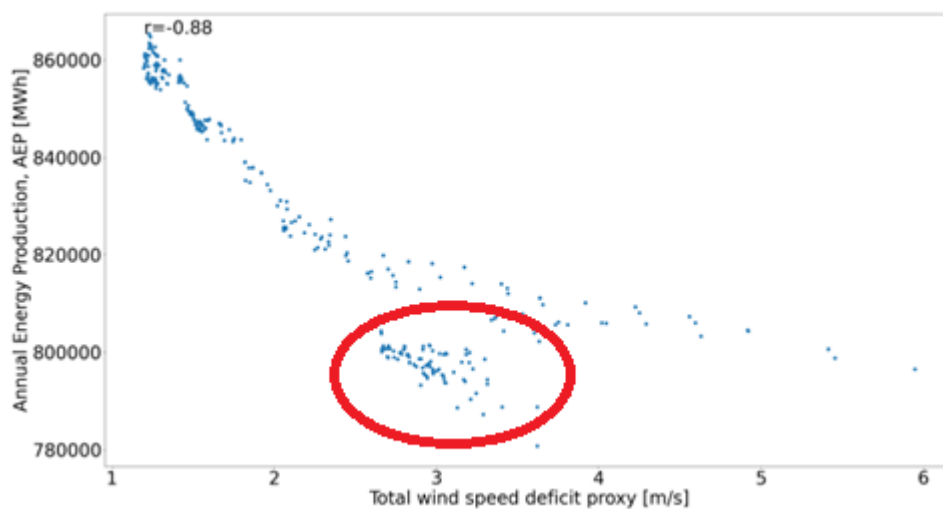
Figure D. Correlation plot AEP vs Linear objective for all solutions in all pools for Case II (total number of feasible points of 412)
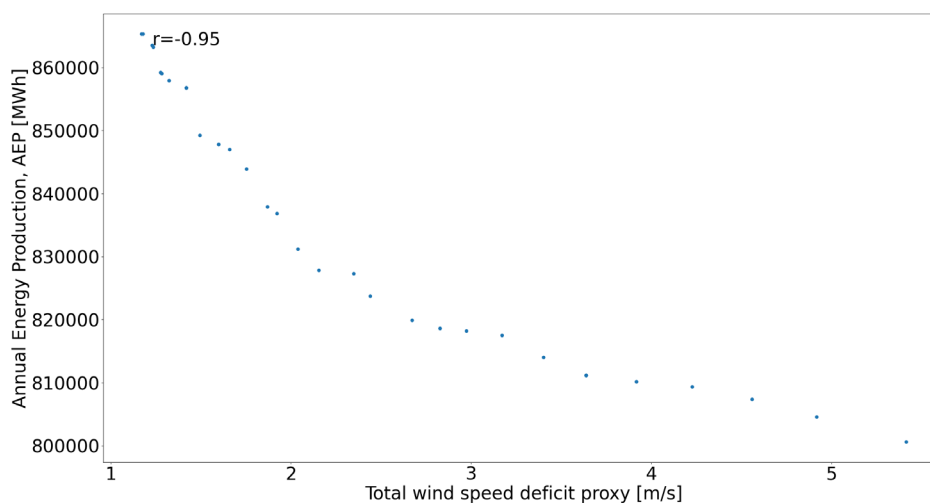
Figure E. Correlation plot AEP vs Linear objective after NSH correction for Case II
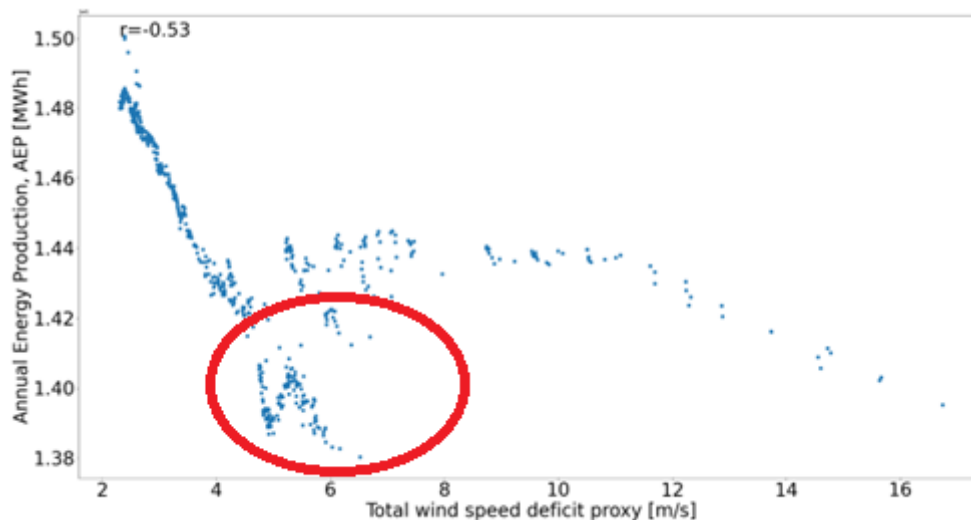
Figure F. Correlation plot AEP vs Linear objective for all solutions in all pools for Case III (total number of feasible points of 714)
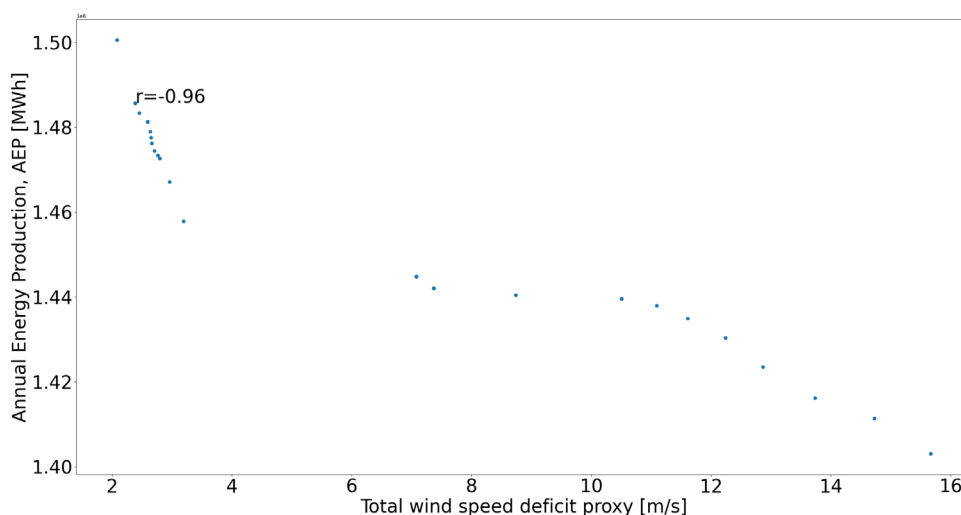
Figure G. Correlation plot AEP vs Linear objective after NSH correction for Case III

The flat parts of Fig. 5, Fig. 7, and Fig. 9 are also due to inability of the heuristics and tree search of the branch-and-cut solver to consistently produce high-quality points (in terms of the proxy objective function), due to the hardness of this kind of combinatorial optimization problems. Furthermore, we think that the sharp improvements of the true objective function (AEP) in the mentioned figures show MILP's added value (and disprove the random search argument). For example, in Case I, when $N = 590$ and $K = 6$ the incumbent is improved more than 1% in less than 20 minutes when four series of MILP runs are solved to optimality. With the number of possible combinations of new solutions for a given incumbent being at least C_3^{574} (31'355,324), we strongly

believe that it would require significant luck for a random search to get quality solutions sampling from a pool of over 31 millions of alternatives in such a short time.

In conclusion, we see that, in general, the correlation between AEP and total wind speed deficit proxy persists.

- <u>MILP modelling contribution:</u> In the introduction (from lines 78 to 87) the works (Turner et al., 2014; Kuo et al., 2016) had been cited, referring to modelling WFLO in integer programming using approximated objective functions. To clearly indicate the positioning of our work, the following are added in the revised manuscript:

  "…This linearization approach is similar to (Turner et al., 2014…" (line 245)

  "…Compared to (Turner et al., 2014), the MILP program (23) with objective replaced by Eq. (24), linearizes the complexity of its largest set of constraints and variables from N^2 to N (Eq. (23b) and Eq. (23e)). Furthermore, the constraints in Eq. (23d), which can lead to infeasible points, are not neglected as in (Turner et al., 2014) …" (line 272 to 274).

- <u>Heuristic algorithm contribution:</u> The use of heuristics is common in the field of integer programming. We had cited the works of (Fischetti et al., 2016; Shaw, 1998) and (Fischetti and Lodi, 2003) as a reference for local branching and neighborhood search theory. The main contribution claimed here is that the presented NSH, that limits the number of changes over binary variables ξ, using solution pool, and exploiting the strong correlation between a proxy (linear) objective function and a true (non-linear) objective function, is novel in the context of WFLO. The NSH is a specific purpose heuristic developed to address the WFLO problem that differs from any of the cited works and the references pointed out by the reviewer. It is hard to see, in our opinion, relevant resemblances with the Random Search of Feng et al. (randomly modifies the position of a single wind turbine at each iteration) and with the Bionic optimization of Song et al. (like the random search). The NSH relies on solving a sequence of MILP models using branch-and-cut (inner heuristics and tree search) to obtain high-quality solutions in terms of an objective function which approximates a true objective to optimize. This allows modifying multiple wind turbines simultaneously for analyzing possible layouts. The DEBO algorithm from *https://wes.copernicus.org/preprints/wes-2022-90* is discussed in the revised version of our manuscript in Introduction and Section 4. The comparisons are highlighted in Red color as this was a suggestion from the   other   reviewer.

  We have added this work in the introduction (paragraph from lines 99 to 109) as "The second main contribution is the proposition of a new special purpose neighborhood search heuristics in order to speed up the generation of high-quality solutions. This heuristic, wrapping both formulations, has a twofold functionality; first to increase tractability, and second to redirect the optimization search in terms of a specified objective function with higher fidelity. Similar neighborhood search methods have been proposed in the literature, as the Discrete exploration-based optimization (DEBO) (Thomas et al., 2022c), which is a two-steps process composed by a greedy initialization and a local search block. While the method proposed in this manuscript shares most of the advantages of the mentioned approach (no gradients required, can handle unconnected and non-convex boundary constraints, and so on), it actually improves the DEBO algorithm as among others, i) significantly less AEP function evaluations are required, and ii) it is based on well-establish integer programming

theory, relying in efficient implementations of the branch-and-cut algorithm. The main numerical results indicate good computational performances for a set of publicly available   benchmark case studies compared to state-of-the-art gradient-free and gradient-based approaches (Baker et al., 2019)."

This article is referred back in this section in paragraph from lines 305 to 307 as

"… One of the advantages of the NSH compared to the DEBO algorithm (Thomas et al., 2022c) is the reduced number of AEP evaluations. In an iteration κ, only $|S|$ evaluations are required. Likewise, many of the other expensive calculations are done in a pre-processing stage…"

"…Another difference between the NSH and the DEBO is that the latter only changes the position of a single WT in a given iteration, while the former considers simultaneous modifications of several WT positions." (lines 312 to 314).

- Computing time reference: Thanks a lot for this feedback. We agree with the reviewer, therefore the statements discussing computing time have been rephrased. The comparison of the NSH with gradient-free methods, including the pseudo-gradient, was rephrased, since the aim was to compare to typical metaheuristics that do not use at all gradients information, as genetic algorithm or swarm optimization, and not to the specific method. Lines 433 to 435 have been modified as
  "…When directly comparing to typical metaheuristics (genetic algorithm, particles swarm optimization, etc), that do not use explicit gradients information, the presented method seems to perform well, being able of determining a similar layout quality in less than 2 h, which is generally faster than average computing time of these kind of algorithms…"
  And lines 463 to 464:
  "…which is generally a reasonable computing time compared to methods where gradients are not explicitly utilized in the optimization process, especially to metaheuristics as genetic algorithm or swarm optimization…"

As a general clarification regarding the computing time of the NSH in Fig. 5, Fig. 7 and Fig. 9, the following paragraph has been modified in the revised manuscript between lines 406 and 412:

"The NSH computing time results in Fig. 5 (blue line) do not reflect the instant where the incumbent is found, but the time progress of this algorithm, which is dependent on the execution of the MILP solver at each iteration. Table 2 contains information about the values of N, K, T, and termination criterion of the solver after each iteration κ of the NSH
Algorithm 1 (beginning from point 2 where $\kappa = 1$). This means that in iterations where the termination criterion is time (and not optimality), one could fine-tune T for an earlier stop, shortening the total time. This is particularly more relevant in cases where internal heuristics of the solver are activated at the root node of the search tree, coming up with the largest portion of solutions very early in the

process. Consequently, the total computing time, for all cases, is conservative and should be taken as an approximated reference."

This paragraph states the real meaning of computing time for the NSH in these figures. We have chosen to show them focusing on trends and potential rather than aiming at exhaustively comparing to all algorithms testbed that use different modelling philosophy and are designed for different purposes.

- Comment: By themselves, the application of a big-M trick to get a more efficient linearization and the design of the NSH are relevant contributions.

That, after the initial part of the optimization runs, more is happening than just a random search, is something that should be demonstrated, because otherwise I feel these contributions are not novel and proven enough to merit acceptance of the paper. The huge computational resources necessary for the piecewise-constant power curve linearization approach leads me to conclude that this approach is impractical, so effectively, that for that approach a negative result has been obtained. That is something that can be reported, but is by itself not enough to merit acceptance.

- Response: We have elaborated in this response letter about the operating principle of the NSH and how this is beyond a random search of a single wind turbine in a given iteration. The main contribution stems from combining the linearization techniques within each MILP model, and the proposition of the NSH wrapping them. For example, the MILP model in Eq. (23) + objective Eq. (24) when solved as a full extensive model performs worse (in terms of final solution quality) than when this is embedded in the NSH (Fig. 5, Fig. 7, and Fig. 9). Conversely, the MILP model Eq. (23) + objective Eq. (24) enhances MILP model Eq. (18) for the fixed WT number case. While we agree that the computational resources are large, we see a great potential in applying them for hard WFLO instantiations, optimization objectives beyond AEP needs, or with complex site-dependent cost functions. Unified optimization with electrical systems would also benefit from this modelling technique. By comparing the results to a large testbed of algorithms, we aim to a proof of concept of the proposed methods, encompassing the MILP models and heuristic, rather than claiming computational superiority against the benchmark studies.

Abstract

- Comment: velocity deficit → wind speed deficit

- Response: Thanks for noticing this imprecision. It has been corrected as suggested.

1: Introduction

- Comment: It is relatively long, so add subsections to help readers see its structured.

- Response: Thanks for the valuable suggestion. We have added subsections within the introduction section as follows: 1.1 Motivation and Problem Definition, 1.2 Optimization Workflow for WFLO, 1.3 Continuous Optimization for WFLO, 1.4 Discrete Optimization for WFLO, 1.5 Literature Review for Integer Programming within WFLO, 1.6 Contributions.

- *Comment*: *l17: turns into a critical task → remains relevant (avoid exaggeration)*

- *Response:* This sentence has been deleted in the new version of the manuscript following a suggestion from the other reviewer. It reads as follows:

"…For wind energy to become the cornerstone of a successful green energy transition, further reduction in costs - partly achievable by economically refined wind farm designs - will play an important role."

- *Comment*: *multiple locations: Authors (Authors, year) → Authors (year) [just use \citet{…}?]*

- *Response:* Thanks for noticing this redundancy. We have fixed it accordingly.

- *Comment*: *l78-89: use list (first, second) to make this paragraph clearer.*

- *Response:* Thanks for the suggestion. In the new subsection 1.6 Contributions this list has been elaborated.

- *Comment*: *l92: Preface with, e.g., "The rest of the paper is structured as follows." for clarity.*

- *Response:* Thanks for the suggestion. We have fixed it accordingly.

- *Comment*: *l93: unfolds → describes? [strange wording]*

- *Response:* Thanks for the suggestion. We have changed this word as recommended.

- *Comment*: *l94: deployed → presented? [strange wording, occurring multiple times]*

- *Response:* Thanks for the suggestion. This work has been replaced by "shown", "depicted", and "introduced" in all the instances where they appeared.

2: Physics Modelling

- *Comment*: *l106: $\delta u\_il → \delta\_il$: for mathematical notation, it is discouraged to use two (multiple) consecutive symbols, as this can be mistaken for the multiplication of two symbols; it also makes the notation heavier than needed.*

- *Response:* Thanks for the suggestion. We have changed this mathematical notation as recommended.

- *Comment*: *l107: mention that it is Case Study 1.*

- *Response:* Done.

- *Comment*: *l109-110: inappropriate paragraph indent after math; avoid by not having blank line? [occurs very often; fix all].*

- *Response*: Done. This type of inaccuracy have been fixed throughout the manuscript.

- *Comment*: *l115: Δu_il → Δ_il (as for δu_il)*

- *Response*: Thanks for the suggestion. We have changed this mathematical notation as recommended.

- *Comment*: *l115: 'wind speed k': the use of k for a wind speed is confusing, as k is typically used for integers, but likely you meant k to be the index for a discretized wind speed value (then make that clear).*

- *Response*: Done. As the reviewer suspects this is referring to a specific index for wind speed in a discretized wind rose. The sentence has been corrected as follows
"…and wind speed index k can be…"

- *Comment*: *l124: drop 'and wind speed k'*

- *Response*: Done

- *Comment*: *l124-125: there is strange extra white space before the displayed equation; check your LaTeX [occurs very often; fix all].*

- *Response*: Thanks for noticing this imprecision. We have fixed it accordingly throughout the manuscript.

- *Comment*: *Eq. 6 is the logical combination rule when one wants a linear objective, but the one of Eq. 7 is used; this needs to be better justified.*

- *Response*: Both superposition models are used. Eq. 6 is used for the power-curve-based model, and while it is also applicable to the power-curve-free model, we have chosen to use Eq. 7 since this optimization model is directly compared to the benchmark study in (Baker et al., 2019), which follows the root sum squares methodology. Thus, results in Sections 5.1, 5.2, 5.3, and 5.4 calculate AEP through Eq. 7 and Section 5.5 uses Eq. 6. Lines 234 to 236 explain this, while repeated in the introduction of Section V, paragraph from lines 320 to 326.

- *Comment*: *l135: only the most simple models of power curves are convex right below rated speed.*

- *Response*: True. An improved description of the power curve has been introduced in the revised manuscript.

- *Comment*: l137: ≤ → < for middle two lines' left-hand inequality

- *Response*: Thanks for noticing this typo. It had been fixed in advance.

- *Comment*: Eq. 9: note that putting the sum over i after the w_jk corresponds to a more efficient calculation

- *Response*: True. Please consider that this is just a representation in the text and does not reflect the actual code implementation.

3: Optimization Models

- *Comment*: l153: '(2D in this study)': mention that when presenting the actual test case, not here.

- *Response*: Done.

- *Comment*: l152: use of j different from wind direction index, so confusing double use of the same symbol; please avoid that.

- *Response*: Thanks for noticing this typo. It has been corrected through the whole manuscript by replacing index j to q used in the distance functions.

- *Comment*: l164: what is meant by 'isometric'? [strange wording]

- *Response*: In this context is used to describe the property of intervals splitting the cubic part of the power curve such as they all have the same length.

- *Comment*: Fig. 1: gray dot hard to see; please improve readability

- *Response*: Done. Colors between the original power curve and the stepwise linear have been swapped.

- *Comment*: Eqs. 16 and 21 would be easier to understand if you first present the set same of equations for the non-linearized way in a grouped way, so that it is easy to see what changes; especially 16f is hard to understand without piecing together some things.

- *Response*: Thanks for the feedback. The sequence of equations describing the characteristics of the sampling method applied to linearize the WT power curve has been extended, in an attempt to improve readability. We do feel though that the wake models inside the MILP formulations are adequately represented. Please note that from lines 223 to 229 the wake model is connected to Eq. (3) and Eq. (6) that in turn expresses the logic process to compute total wind speed at a given location.

- Comment: Eq. (16b): wouldn't ξ_i+sum_{j in N_i}ξ_j≤1 for all i be a more efficient set of constraints?

- Response: Unfortunately, not. Note that in ξ_i+sum_{j in N_i}ξ_j≤1 if a ξ_j=1, then all ξ_l such as l in N_i and j ≠l will be forced to be zero, but not necessarily the condition d_{jl}<d^min would be satisfied, because the set N_i contains elements satisfying this
condition with respect to i. Therefore, it is mandatory that this constraint is N^2 in worst-case.

- Comment: l205: necessitated → needed

- Response: Thanks, done.

- Comment: l206: total wind speed → sum of wind speeds ('total' was confusing to me here)

- Response: Done.

- Comment: l211: 'dropping the square roots' is a very crude way of introducing the linearization of the square root here; explain why you use this expression and not one with a different coefficient (you could also just put an abstract coefficient in front and drop it when you drop the first term).

- Response: We acknowledge that simply dropping the square roots the model is not "correct", but expect that the resultant expression, incorporated in the MILP model, is "good enough".
Line 244 is added:
"…the arguments of the square roots in Eq. (19) define a function closely related to the full root-squared expression…"
To have a better idea about this premise, please see the below plot
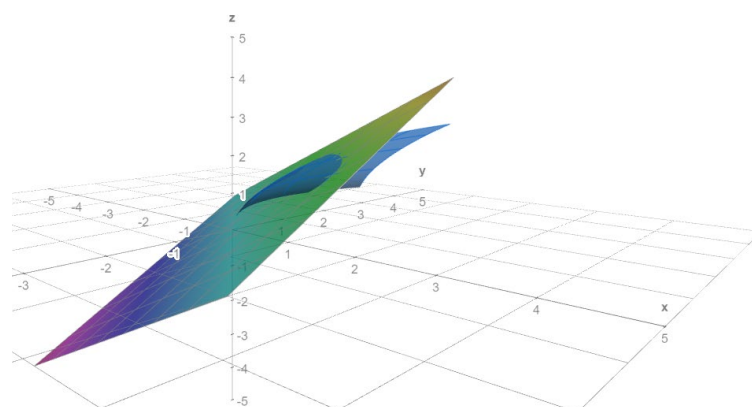
The plane plot is of the function $z = x + y$ and the other one is for $z = \sqrt{x} + \sqrt{y}$. Note how these two functions follow relatively close to each other for non-negative values of x and y. A

similar behavior is expected between the original root-squared expression and the one that ignores them. Practical evidence of the accuracy of this simplification is presented in Table 1.

- *Comment:* l221: provide reference for big-M trick

Response: Done.

4: Neighborhood Search Heuristic

- *Comment:* Alg.1 line 11: This is the first time 'solution pool' appears; this concept needs to be introduced on beforehand and it needs to explained concretely which solutions are in this pool and how they are generated (this is for me the part of the explanation that endangers reproducibility the most for me).

- *Response:* Thanks for pointing this out. The following explanation of the solution pool has been added in lines 300 to 302.
"After solver termination, the solution pool S is retrieved in line 11. The solution pool contains all the feasible layouts obtained in an iteration κ from the MILP solver. These points are a result of a linear programming relaxation or from applying heuristics in a given node, such as, relaxation induced search, polishing, and feasibility pump (IBM, 2022)…"

5: Computational Experiments

- *Comment:* l288: V used in a second meaning from in Alg.1; avoid reusing mathematical symbols.

- *Response:* Thanks for pointing out this redundancy. V for the number of wind speeds has been replaced by \Upsilon.

- *Comment:* l330: relation between U and Ũ: not very interesting, rather between AEP and Ũ would be.

- *Response:* This is exactly presented in Fig. 4c but instead of Ũ the component linked to deficit is plotted. A graph between AEP and Ũ would simply have a positive slope with same correlation.

- *Comment:* l363: 'The inputs are tuned …': please share how this was done and how much effort this entails.

- *Response:* This discussion has been extended in lines 392 to 405. The framework seems robust for wide internals of tunned values of these parameters, the presented here were obtained after few trial and error attempts.

- *Comment*: l365: seek → search

- Response: Thanks for the advice. Done.

- Comment: *The use of % in the discussion of 5.2-4 is confusing; a better approach is to use wake loss factor/percentage (1-AEP/AEP_wakeless) and mention percentage point changes; wake loss factor (differences) are independent of the starting layout and provide the scale of things that are of interest to wind farm developers (a 1 percentage point difference in wake loss factor is practically significant, but a 0.1 percentage point difference likely not anymore, as it will likely be below the uncertainty bounds*
involved due to model uncertainty); wake loss factors can also be compared across wind farms, as they do not depend on the number of turbines.

- Response: We do not really see a big added value by transforming the presented percentages from ((AEP_step/AEP_lastcommentedstep)-1) to (1-AEP_step/AEP_wakeless). The choice of showing this percentage calculation is to put it in the same context as the performance plots in Fig. 5, Fig. 7, and Fig. 9, which are presenting AEP vs computing time, while evaluating the improvement over a time slot.

- Comment: *There are numbers with 8 significant digits listed (some AEP values), which is absurd, as modelling inaccuracies make such precision unrealistic; try to give all numbers with a reasonable number of significant digits (giving more than 3 or 4 is typically dubious).*

- Response: We have corrected these numbers accordingly.

- Comment: *Figs. 5, 7, 9: put yellow box material in table for better legibility.*

- Response: Done.

- Comment: *l385: escalates → scales.*

- Response: Done.

- Comment: *l420-422: regarding the pattern in NSH operation: you cannot conclude what you have stated, as you always use smaller neighborhoods before larger ones; making statements like this would require comparison at least with runs where the neighborhood size decreases; I would just leave out this statements.*

- Response: Done.

- Comment: *l451: you state that the power curve-free approach is not suited for NPV optimization, but as part of the linearization, it is entirely possible to estimate a coefficient to transform (m/s)² to units of currency; so I find the current argumentation to a be a bit limited; I'd suggest including a more nuanced argumentation.*

- Response: We are very aware of this possibility. Such a linearization would require performing a single variable linear regression mapping wind speed to units of currency. It is very important in this approach to properly weight both cost components (cost of wind turbines and energy revenues) for the optimization not to be ill-conditioned. We have elaborated the following correlation plot for a case of variable number of wind turbines (ranging from 10 to 100) using the power-curve-free model:
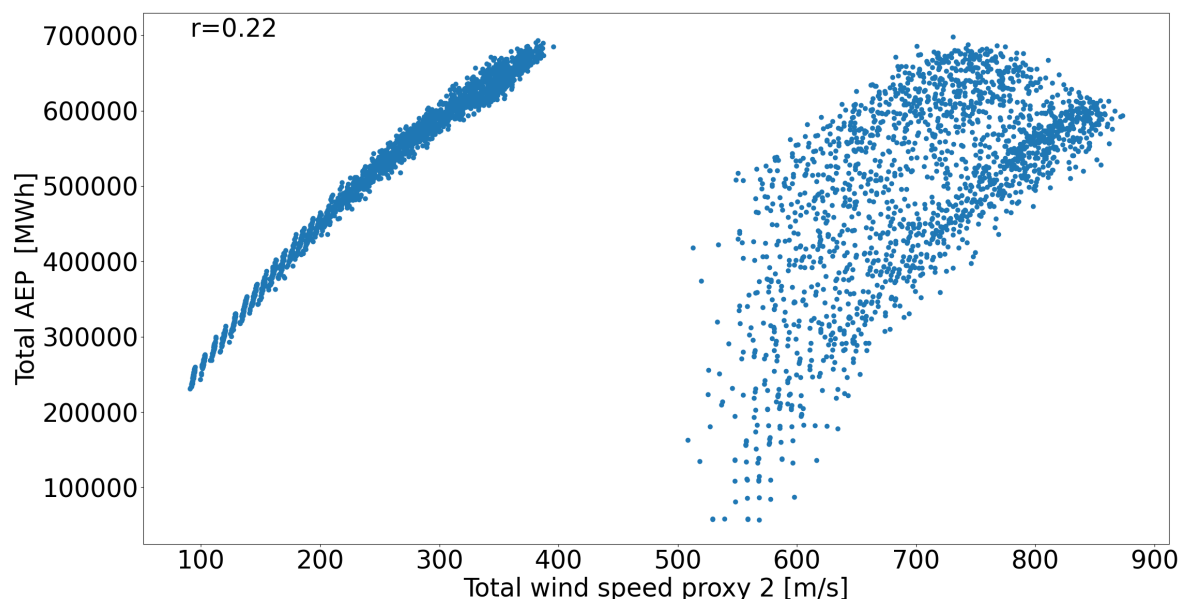
From the plot, one can conclude that in some cases there could be a good correlation between AEP and total wind speed deficit, however in other cases the correlation is quite poor. If one "hits" the case situate on the left side of the plot, the mapping could give good results, however this would be rather random. The following statement has been added between lines 486 and 490.

"…Even if the power-curve-free model (Sect. 3.2) exhibits a quite good performance in terms of AEP and computing time for fixed number of WTs (when AEP and NPV are basically the same metric), it is not very well suited when variable number of wind turbines are considered. Based on computational experiments not included in the paper, the power-curve-free model embedded in the NSH terminates too early in the search process, resulting in a worse solution than the alternative discussed in the following…"

- Comment: *l463: 'Mill.Eur' is not a proper unit; please use proper units also for currencies.*

- Response: We have chosen to replace 'Mill. Eur' by m EUR according to https://publications.europa.eu/code/en/en-370303.htm#:~:text=10%20bn%20GBP-,NB%3A,is%20insufficient%20for%20spelling%20out.

6: Discussion

- Comment: l499-500: Is it hard to establish whether a MILP formulation would still be possible? As long as the wake model enters into the picture via pairwise deficits, it should work without material changes.

- Response: We refer to the fact that the thrust coefficient is function of the local turbine wind speed, which in turn affects the pairwise deficits. In a MILP formulation these deficits are computed in advance if the program is extensively formulated as a fully compact model. Then, it is not possible to calculate them in function of the local speed before knowing the positioning of the wind turbines. Strategies as lazy constraint callbacks may be handy for this issue, but we have not done the corresponding rigorous analysis to determine with certainty at what extent this is accurate.

- Comment: l507-508: Why hasn't the study for the dependence on initial layout been done yet? As far as I understand, it is mostly just a matter of rerunning the cases n times. (While I understand that this takes time, the optimization runs would not require full convergence, but just long enough to see repeated/varying behavior.) This would be an interesting addition to the paper and increase its value.

- Response: We place this analysis as an extra study to be formally addressed and presented in subsequent research, as the emphasis of this article has been into describing the proposed integer programming models and the heuristics. We do not expect that by changing initial layouts, the final solution will be markedly changed and typically linear integer programming models are not as dependent to the initial layout as gradient-based methods. Considering the actual article length (32 pages), this extra content may not get sufficient attention, as other very important points as both integer linear programs, correlation analysis, NSH operation, global model performance analysis, and non-classic WFLO have been prioritized. To avoid confusions, we have removed the future work part from the manuscript.

We strongly believe that the manuscript has gained strength, consistency, coherence, and formality by the changes suggested by the Reviewers. We thank them and look forward to hearing from them again.

Best wishes,
Juan-Andrés Pérez-Rúa
Mathias Stolpe
Nicolaos A. Cutululis

A Neighborhood Search Integer Programming Approach for Wind Farm Layout Optimization

Juan-Andrés Pérez-Rúa[1], Mathias Stolpe[1], and Nicolaos Antonio Cutululis[1]

[1] Department of Wind and Energy Systems, Technical University of Denmark, Frederiksborgvej 399, 4000 Roskilde, Denmark

Correspondence: Juan-Andrés Pérez-Rúa (juru@dtu.dk)

Abstract. Two models and a heuristic algorithm to address the wind farm layout optimization problem are presented. The models are linear integer programming formulations where candidate locations of wind turbines are described by binary variables. One formulation considers an approximation of the power curve by means of a step-wise constant function. The other model is based on a power-curve-free model where minimization of a measure closely related to total wind speed deficit is optimized. A special-purpose neighborhood search heuristic wraps these formulations increasing tractability and effectiveness compared to the full model that is not contained in the heuristic. The heuristic iteratively searches neighborhoods around the incumbent using a branch-and-cut algorithm. The number of candidate locations and neighborhood sizes are adjusted adaptively. Numerical results on a set of publicly available benchmark problems indicate that a proxy for total wind speed deficit as objective is a functional approach, since high-quality solutions of annual energy production metric are obtained, when using the latter function as substitute objective. Furthermore, the proposed heuristic is able to provide good results compared to a large set of distinctive approaches that consider the turbine positions as continuous variables.

1 Introduction

1.1 Motivation and Problem Definition

Cost reductions for renewable energy generation is on the top of political agendas, with the objective of supporting the worldwide proliferation of clean energy production systems. Subsidy-free tendering processes become more frequent, as is the case for offshore wind auctions in Germany since 2017 and in Netherlands since 2018, or in China for onshore wind from 2021 (GWEC, 2020a). The fast evolution of offshore wind in the last decade, with a sharp growth of global installed capacity (GWEC, 2020b), is yet another clear indicator of growth trend of wind energy. For wind energy to become the cornerstone of a successful green energy transition, further reduction in costs - partly achievable by economically optimized wind farm designs - will play an important role.

The basic Wind Farm Layout Optimization (WFLO) problem aims at deciding the positioning of Wind Turbines (WTs) within a given project area to maximize the Annual Energy Production (AEP), while respecting a minimum separation distance. The classic problem definition aims at placing a fixed number n_T of typically homogeneous (single type) WTs. This problem has been studied broadly and intensively since at least three decades (Herbert-Acero et al., 2014). The first effort in the topic

1

was the pioneering work of Mosetti et al. (1994), where the Katic-Jensen wake decay model (Katic et al., 1986), implemented to compute wake losses, is coupled with a genetic algorithm as optimizer to iteratively improve the layout.

1.2 Optimization Workflow for WFLO

The main components when building an optimization workflow for the WFLO problem are the wake models (deficit and superposition), the program formulation, and the associated numerical algorithms. For formulating tractable frameworks, the designer needs to rely on the so-called engineering wake models. These are essentially mathematical representations which can be expressed in terms of analytical equations after significantly simplifying complex physics modelling, while still capturing to a good extent the underlying nature of the phenomenon under analysis. Scientific articles in this field have proposed and validated engineering wake models with smooth and differentiable velocity deficit shape, two examples are the Bastankhah's Gaussian (Bastankhah and Porté-Agel, 2016) or its simplified version (IEA Wind Task 37, 2019), and the Jensen cosine model (Jensen, N.O., 1983). Likewise, the aggregation of individual wake velocity deficits can be done through linear superposition (Lissaman, 1979) or root sum squares (Voutsinas et al., 1990), with local or freestream velocity conditions (Porté-Agel et al., 2020).

1.3 Continuous Optimization for WFLO

Optimization techniques for the WFLO problem formulation can be classified, depending on the choice of variables, into continuous and discrete optimization. In the field of continuous optimization, the location $\mathbf{p}_i$ of a WT i, in terms of the abscissa (x_i) and ordinate variables (y_i) in the Cartesian plane, $\mathbf{p}_i = (x_i, y_i)$, can take any real values, while ensuring that the point is within the project area $\mathbf{F}$, and simultaneously satisfying the minimum distance constraints. Several gradient-free algorithms have been applied to this problem, including metaheuristics, as genetic algorithm (Réthoré et al., 2014) or particle swarm optimization (Wan et al., 2010). Likewise, gradient-based methods can be used, as for example the Sparse Nonlinear OPTimizer (SNOPT), that uses a Sequential Quadratic Programming (SQP) approach (Thomas et al., 2022a), or interior-point solvers (Pérez et al., 2013). In general, gradient-free algorithms, although highly flexible for modelling aspects, have considerably poorer scalability for larger problem sizes than gradient-based approaches. Re-parametrization approaches aiming to reduce the number of variables through simplified geometrical representations of the problem, such as row and column spacing or inclination angle, are also emerging (Stanley and Ning, 2019). Additionally, multi-start strategies are frequently implemented as a workaround for the intrinsic multi-modal nature of the WFLO problem. Finally, hybrid methods combining gradient-free and gradient-based algorithms have been proposed with good results (Mittal and Mitra, 2017).

The utilization of simplified objective functions closely related to more sophisticated AEP models is also an emerging research field for continuous gradient-based optimization. In the recent work (LoCascio et al., 2022), a novel formulation for time-averaged wake velocity incorporating an analytical integral of wake deficits across wind direction is proposed. This article shows the application of this analytical formulation for WFLO using the Sequential Least Squares Quadratic Programming (SLSQP) as numerical algorithm. Computational results indicate the ability of this approach in finding WT layouts with energy production comparable to the alternative of optimizing directly more accurate AEP objectives.

1.4 Discrete Optimization for WFLO

Discrete optimization models can be formulated for this problem by means of sampling the available project area in form of N candidate location points. Thus, only a set of finite options from the continuous search space are considered, where the n_T WTs to be installed are in principle $n_\text{T} \ll N$. In contrast to continuous optimization, a candidate point i is then represented by a binary variable ξ_i, that gets a value of one if a WT is installed at that location, or zero otherwise. The vast majority of articles in the literature implement gradient-free algorithms for this technique, as the works of Mosetti et al. (1994) and Grady et al. (2005), both using genetic algorithms. Algorithms utilizing explicit gradients are also a valid approach in this field (Pollini, 2022). This modelling technique fits very well in the well-studied general framework of integer programming. The main advantage of this approach is the possibility to utilize exact solvers based on branch-and-cut method; theoretically able to solve a problem to optimality while supporting common engineering constraints (Wolsey, 2020). Nevertheless, the low tractability and poor scalability of this method as function of the size of N and the number of state variables is well-known.

A large number of benefits are implicit in the discrete modelling technique over the continuous counterpart, including: (i) capacity to include the number of WTs as a variable and to model overall economic metrics as Net Present Value (NPV), (ii) ease of modelling any shape of project area or forbidden zones, convex or non-convex, (iii) capacity to model extensive integrated models to support electrical systems optimization, (iv) ease of modelling terrain-based constraints or cost functions, (v) ease of incorporating multiple WT types, among others. These functionalities are the main motivation for focusing on proposing new methods for the WFLO problem in the area of discrete optimization. Moreover, in broader terms, since even the basic definition of the WFLO problem translates into a non-convex formulation, new methods are required to efficiently obtain high-quality solutions.

1.5 Literature Review for Integer Programming within WFLO

Probably the first work within the context of integer programming for the WFLO problem was the thesis of Fagerfjäll in 2010 (Fagerfjäll, 2010), where a Mixed Integer Linear Program (MILP) is proposed, modelling the objective AEP function as a superposition of deficits defined in terms of power. Although physically inaccurate, as the deficit superposition should be computed for velocities, an important reduction in the number of variables is achieved that ultimately allow solving to optimality rather small problem instances. A similar approximation is carried out by Archer et al. (2011), Fischetti et al. (2016), and Quan and Kim (2019), but introducing important modifications to the model by reducing number of constraints. The objective function may also be formulated for aggregated velocity deficit (Turner et al., 2014; Kuo et al., 2016), but the imperfect correspondence with AEP will result in not solving to optimality, possibly resulting in final low-quality solutions. Another advantage of integer programming formulations is the chance of incorporating heuristic routines in the top of such models, as for instance proximity search (Fischetti et al., 2016; Shaw, 1998), to quickly improve a given starting feasible point.

1.6 Contributions

Several contributions to the field of discrete optimization for WFLO are proposed in the manuscript. The first contribution is the proposition of new integer linear formulations which are able to capture to a good extent the underlying physics of the problem. The main obstacles for a MILP representation of WFLO problem are the non-linearity of the power curves, and the choice of wake velocity deficit superposition approach. Currently, the scientific literature has fundamental knowledge gaps. For example, previous works have considered aggregation of power deficits instead of velocities, gaining a simplification on the mathematical formulation in detriment of the physics modelling fidelity. This manuscript presents new strategies for modelling both facets in the class of MILP problems, one with explicit power curve and wake superposition modelling, and another with a proxy objective function based on total wind speed, thus simplifying the original formulation. In contrast to (LoCascio et al., 2022), this proxy objective is developed for MILP optimization, meaning that the aim is to get a linear expression that does not need to be friendly for explicit gradient-based optimization.

The second main contribution is the proposition of a new special purpose neighborhood search heuristics in order to speed up the generation of high-quality solutions. This heuristic, wrapping both formulations, has a twofold functionality; first to increase tractability, and second to redirect the optimization search in terms of a specified objective function with higher fidelity. Similar neighborhood search methods have been proposed in the literature, as the Discrete exploration-based optimization (DEBO) (Thomas et al., 2022c), which is a two-steps process composed by a greedy initialization and a local search block. While the method proposed in this manuscript shares most of the advantages of the mentioned approach (no gradients required, can handle unconnected and non-convex boundary constraints, and so on), it actually goes beyond the DEBO algorithm as among others, i) significantly less AEP function evaluations are required, and ii) it is based on well-establish integer programming theory, relying in efficient implementations of the branch-and-cut algorithm. The main numerical results indicate good computational performances for a set of publicly available benchmark case studies compared to state-of-the-art gradient-free and gradient-based approaches (Baker et al., 2019).

The rest of the manuscript is structured as follows. Section 2 introduces the engineering models of the physical aspects of interest. Section 3 presents the two mathematical programs developed, and Sect. 4 describes the proposed heuristic framework wrapping both programs. Computational experiments are shown in Sect. 5, followed up by discussions in Sect. 6, and lastly the manuscript is finalized with the conclusions in Sect. 7.

2 Physics Modelling

The proposed MILP models and general optimization framework in this manuscript can be easily applied to many wake deficit models. No particular properties on smoothness or differentiability are required from these models for optimization purposes. Additionally, no specific demands on mathematical structure in connection with controlling wake diameter and deficit (Thomas et al., 2022b) are stemming from the optimization programs proposed in this article. Since the computational results in the article are obtained after solving open access case studies from the IEA Wind Task 37 (Baker et al., 2019), the wake model implemented there is presented in Sect. 2.1, along with the superposition techniques in Sect. 2.2, WT power curve in Sect.

2.3, and the AEP calculation procedure in Sect. 2.4. Variations on ways of computing the absolute velocity deficits and linear wakes superposition under the framework of MILP are also introduced.

2.1 Wake Deficit Model

A simplified version of the Bastankhah's Gaussian is considered (IEA Wind Task 37, 2019). The relative velocity deficit $\delta_{i\ell} = \Delta_{i\ell}/u_\infty = (u_\infty - u(\bar{x}_i, \bar{y}_i))/u_\infty$ behind a single WT located at ℓ, and evaluated at point i, is described using the model and notation from Case Study I (IEA Wind Task 37, 2019).

$$\delta_{i\ell} = \begin{cases} \left(1 - \sqrt{1 - \frac{C_{\mathrm{T}}}{8\sigma_{\mathrm{y}}^2/D^2}}\right) \exp\left(-0.5\left(\frac{\bar{y}_i - \bar{y}_\ell}{\sigma_{\mathrm{y}}}\right)^2\right), & \bar{x}_i - \bar{x}_\ell > 0 \\ 0, & \text{otherwise.} \end{cases} \tag{1}$$

$$\sigma_{\mathrm{y}} = k_{\mathrm{y}}(\bar{x}_i - \bar{x}_\ell) + D/\sqrt{8} \tag{2}$$

where u_∞ is the inflow wind speed, C_{T} is the thrust coefficient, $\bar{x}_i - \bar{x}_\ell$ is the stream-wise distance from the hub generating wake ($\bar{x}_\ell$) to hub of interest ($\bar{x}_i$) along freestream (let this difference be $d_{i\ell}^{\parallel}$), $\bar{y}_i - \bar{y}_\ell$ is the span-wise distance from the hub generating wake to hub of interest perpendicular to freestream (let this difference be $d_{i\ell}^{\perp}$), σ_{y} is the standard deviation of the wake deficit, k_{y} is a variable based on a turbulence intensity, and D is the WT diameter.

2.2 Wake Velocity Deficit Superposition Model

The absolute velocity deficit $\Delta_{i\ell}(\theta^j, k)$ at wind direction θ^j and wind speed index k can be estimated in two ways. Either based on the inflow wind speed (Lissaman, 1979; Katic et al., 1986) through

$$\Delta_{i\ell}(\theta^j, k) = \delta_{i\ell}(\theta^j, k)u_\infty^k \tag{3}$$

or based on the wind speed $u_{\ell j k}$ at WT ℓ creating the wake at point i for wind direction θ^j and speed k (Voutsinas et al., 1990; Niayifar and Porté-Agel, 2015),

$$\Delta_{i\ell}(\theta^j, k) = \delta_{i\ell}(\theta^j, k)u_{\ell j k} \tag{4}$$

here $\delta_{i\ell}(\theta^j, k)$ is the relative velocity deficit of ℓ over i at operation condition $\{j, k\}$ after Eq.(1) and Eq.(2). Note that Eq. (3) leads to a greater value and therefore is considered a conservative approach compared to (the potentially more realistic) Eq. (4). Nonetheless, implementing Eq. (3) greatly simplifies the resultant system of equations and allow for preprocessing calculations.

Let the set $\boldsymbol{U}_i^{\theta^j}$ collects the WTs creating wake over WT at point i for wind direction θ^j as per

$$\boldsymbol{U}_i^{\theta^j} = \{\ell \mid \text{position } \ell \text{ is up-wind compared to position } i \text{ for wind direction } j\} \tag{5}$$

the wake velocity deficit superposition, to calculate the total velocity deficit at WT i, $\Delta_i(\theta^j, k)$, can be obtained through two mechanisms. Either it is based on linear superposition model (Lissaman, 1979; Niayifar and Porté-Agel, 2015) through

$$\Delta_i(\theta^j, k) = \sum_{\ell \in \boldsymbol{U}_i^{\theta j}} \Delta_{i\ell}(\theta^j, k) \tag{6}$$

or it is based on the root sum squares superposition model (Katic et al., 1986; Voutsinas et al., 1990)

$$\Delta_i(\theta^j, k) = \sqrt{\sum_{\ell \in \boldsymbol{U}_i^{\theta j}} \Delta_{i\ell}^2(\theta^j, k)} \tag{7}$$

2.3 WT Power Curve

Suitable power curves are required for computing AEP. Often, power curves are not perfectly suitable for optimization, due to the usual non-differentiability in several points throughout the function. Generally, a power curve is zero below cut-in wind speed, zero above the cut-out wind speed, and constant between the rated wind speed and the cut-out wind speed. In this particular study, between the cut-in and rated wind speeds the curve is assumed to be smooth, convex and monotonically increasing. The simplified power curve for a generic turbine as a function of wind speed u is modelled through

$$p(u) = \begin{cases} 0, & u < u^{\text{cut-in}} \\ p^{\text{rated}} \left(\frac{u - u^{\text{cut-in}}}{u^{\text{rated}} - u^{\text{cut-in}}} \right)^3, & u^{\text{cut-in}} \le u < u^{\text{rated}} \\ p^{\text{rated}}, & u^{\text{rated}} \le u < u^{\text{cut-out}} \\ 0, & u \ge u^{\text{cut-out}}. \end{cases} \tag{8}$$

where p^{rated} is the nominal power at (and above) rated wind speed u^{rated}. The other turbine characteristics are the cut-in wind speed $u^{\text{cut-in}}$, and the cut-out wind speed $u^{\text{cut-out}}$. In this definition, the WT power curve is not differentiable at $u^{\text{cut-in}}$, u^{rated}, $u^{\text{cut-out}}$, since in these points the left and right hand side derivatives are different. Be aware that the optimization programs proposed in this manuscript are not dependent on WT power curve differentiability.

2.4 Annual Energy Production, AEP

The AEP is calculated with

$$AEP = 8760 \sum_{i=1}^{n_{\text{T}}} \sum_{j,k} w_{jk} p(u_{ijk}) \tag{9}$$

where w_{jk} is the joint probability of wind direction j and wind speed k, and 8760 is the number of hours of a standard year.

3 Optimization Models

The MILP program with explicit modelling of the WT power curve, wake deficit, and wakes superposition, is introduced in Sect. 3.1. Then, the power-curve-free formulation is described in Sect. 3.2.

The main type of variables $\xi_i \in \{0,1\}$ represent presence or absence of turbines at the candidate locations, for both models. Given N points, i.e. candidate locations for turbine positions, with positions $\mathbf{p}_i$ inside the domain $\mathbf{F}$ (i.e. $\mathbf{p}_i \in \mathbf{F}$ for all i WT candidate locations), binary variables $\xi_i \in \{0,1\}$ are associated with the following interpretation

$$\xi_i = \begin{cases} 1, & \text{if a turbine is located at point } i \text{ with position } \mathbf{p}_i, \text{ and} \\ 0, & \text{otherwise.} \end{cases} \tag{10}$$

Let the index sets $\mathbf{N}_i$ storing the candidate locations violating the minimum distance constraints for a WT i be defined as

$$\mathbf{N}_i = \{q \in \{1,\dots,N\}, q \neq i \mid d_{iq}(\mathbf{p}_i, \mathbf{p}_j) < d^{\min}\} \tag{11}$$

where $d^{\min} > 0$ is the minimum required distance between two turbines. If $\xi_i = 1$ then all binary variables in the set $\mathbf{N}_i$ should be forced to zero, whereas if $\xi_i = 0$ these variables should be free to take any value in $\{0,1\}$.

All relevant distances can be pre-processed for all combinations of points i and q. These parameters are then defined as function of the Cartesian plane positions $\mathbf{p}$ and wind direction θ^j, as the Euclidean distances $d_{iq}(\mathbf{p}) = \|\mathbf{p}_i - \mathbf{p}_q\|_2$, the stream-wise distances $d_{iq}^{\parallel}(\mathbf{p}; \theta^j)$ and the span-wise distances $d_{iq}^{\perp}(\mathbf{p}; \theta^j)$, extending the concept introduced in Sect. 2.1.

3.1 Power-curve-based Model

Continuous state variables u_{ijk} are used for wake modelling and power computation. A variable u_{ijk} represents the wind speed at WT location i, for wind direction j, and wind speed k.

The power curve is approximated with a step-wise function. The cubic part of the power curve is first partitioned into m intervals, plus one interval from a negative point $(-u^{\text{ini}})$ to the cut-in speed, and a final one to cover the range from rated to cut-out speed. Each isometric interval within the cubic domain of length $\Delta u = (u^{\text{rated}} - u^{\text{cut-in}})/m$, is approximated with a constant power value, see Fig. 1.

An interval l of the whole domain is characterized by three parameters u_s^l, u_m^l, and u_h^l with the next properties

$$u_s^1 = -u^{\text{ini}}, u_h^1 = u^{\text{cut-in}}, u_s^{m+2} = u^{\text{rated}}, u_h^{m+2} = u^{\text{cut-out}} \tag{12}$$

$$u_s^2 = u^{\text{cut-in}}, u_h^{m+1} = u^{\text{rated}} \tag{13}$$

$$u_s^{a+1} = u^{\text{cut-in}} + (a-1)\Delta u \text{ for } a = 1,\dots,m \tag{14}$$

$$u_h^{a+1} = u^{\text{cut-in}} + a\Delta u \text{ for } a = 1,\dots,m \tag{15}$$

7

$$u_{\mathrm{m}}^l = 0.5(u_{\mathrm{s}}^l + u_{\mathrm{h}}^l) \tag{16}$$

Figure 1. Piece-wise constant approximation of a wind turbine power curve through sampling with $m = 10$ intervals between the cut-in and rated wind speeds.

Equation (12) defines the lower and upper limits for the extreme intervals $l = 1$ and $l = m+2$, Eq. (13) formalizes the lower and upper limits for the first interval in the cubic part, $a = 1$, and the last one $a = m$, respectively. Equation (14) expresses the lower limits for intervals in the cubic part ($a = 1, \ldots, m$), while Eq. (15) does it for the upper limits. Equation (16) presents how to determine the extracted wind speed associated to the interval l of within whole domain, which is the average value of u_{s}^l and u_{h}^l.

Let define the binary state variables $\eta_{ijk}^l \in \{0,1\}$ for $l = 1, \ldots, m+2$ with the interpretation

$$\eta_{ijk}^l = \begin{cases} 1, & \text{if } u_{\mathrm{s}}^l \le u_{ijk} \le u_{\mathrm{h}}^l, \text{ and} \\ 0, & \text{otherwise.} \end{cases} \tag{17}$$

i.e. these variables indicate which of the wind speed intervals l of the power curve approximation for WT i, operates at wind direction j, and wind speed k.

With all the variables of the model - activation variables ξ, continuous state variables u, and binary state variables η - introduced, formulation in Eq. (18) collects the AEP objective function, the constraints of a generalized version of the WFLO problem, and the variables' domain definition.

8

$$\underset{\xi,\eta,u}{\text{maximize}}\ 8760\sum_{i=1}^{N}\sum_{j,k}\sum_{l=1}^{m+2} w_{jk}\eta_{ijk}^{l}p(u_{\mathrm{m}}^{l}) \tag{18a}$$

$$\text{subject to: } \xi_i + \xi_q \leq 1 \qquad\qquad \forall\, i, q \in \boldsymbol{N}_i \tag{18b}$$

$$n^{\min} \leq \sum_{j=1}^{N} \xi_j \leq n^{\max} \tag{18c}$$

$$\sum_{l=1}^{m+2} \eta_{ijk}^{l} u_{\mathrm{s}}^{l} \leq u_{ijk} \leq \sum_{l=1}^{m+2} \eta_{ijk}^{l} u_{\mathrm{h}}^{l} \qquad\qquad \forall\, (i,j,k) \tag{18d}$$

$$\sum_{l=1}^{m+2} \eta_{ijk}^{l} = 1 \qquad\qquad \forall\, (i,j,k) \tag{18e}$$

$$u_{ijk} = u_{\infty}^{k}\big(\xi_i - \sum_{\ell \in \boldsymbol{U}_i^{\theta^j}} \xi_\ell \delta_{i\ell}(\theta^j, u_{\infty}^k)\big) \qquad\qquad \forall\, (i,j,k) \tag{18f}$$

$$\xi, \eta \in \{0,1\} \quad u \in \mathbb{R} \tag{18g}$$

the objective function in Eq. (18a) is an approximation of the AEP computation presented in Eq. (9). Equation (18b) models the minimum distance constraints as explained in the introduction of Sect. 3. If a binary variable ξ_i is active, then all candidate points closer than $d^{\min}$ should be excluded, i.e. set to zero. If a binary variable ξ_i is inactive then the other candidates are still eligible. The definition of the set $\boldsymbol{N}_i$ is provided in Eq. (11). Equation (18c) models the situation that the designer requires at least $n^{\min}$ and at most $n^{\max}$ WTs to be located in the domain. Note that for the classic problem definition $n^{\min} = n^{\max} = n_{\mathrm{T}}$. Equation (18d) connects state variables u and η as explained in Eq. (17) while Eq. (18e) forces one operation case active for each WT candidate at each wind direction and speed. The last constraint in Eq. (18f) is for the wake velocity deficit and wakes superposition modelling to calculate wind speed for each candidate location at each wind direction and inflow speed u_{∞}^k. The presented model supports a conservative velocity deficit approach (Eq. (3)) with linear superposition (Eq. (6)). The definition of set $\boldsymbol{U}_i^{\theta^j}$ is provided in Eq. (5). Note that an extension, consisting in creating extra continuous state variables and associated constraints, could allow for considering the more realistic approach in Eq. (4). It is still unknown if the root sum squares model of Eq. (7) could be implemented in the framework of MILP. Finally, Eq. (18f) defines the domain of the required variables. A value for u^{ini} of $u^{\text{cut-out}}$ is set up.

3.2 Power-curve-free Model

Albeit the formulation of Sect. 3.1 represents to a very large extent the physics ruling the problem, it has a considerable number of variables and constraints that may hinder the capacity to tackle larger problems. The model presented in this section neglects power curve and AEP calculation and aims at simplifying the power-curve-based version.

The model introduces a strategy to account for the combination of Eq. (3) and Eq. (7) to calculate velocities, since the case studies from the IEA Wind Task 37 follow this methodology for AEP computation. It would be possible though to consider the linear superposition model if necessary. However, the power-curve-free model does not support the application of Eq. (4).

Combining Eq. (3) and Eq. (7) and extending the summation range in Eq. (7) to all candidate locations, the sum of wind speeds in the farm, U, can be modelled through

$$U = \sum_{i=1}^{N}\sum_{j,k} w_{jk} u_{\infty}^{k} \xi_i - \sum_{i=1}^{N}\sum_{j,k} w_{jk} u_{\infty}^{k} \sqrt{\sum_{\ell=1}^{N}(\delta_{i\ell}(\theta^j, u_{\infty}^k))^2 z_{i\ell}} \tag{19}$$

where new binary variables $z_{i\ell}$ are introduced. The variable $z_{i\ell}$ is equal to one if both WTs i and ℓ are active (i.e. if $\xi_i = \xi_\ell = 1$) and zero otherwise. Nevertheless, the previous expression is not linear for variable $z_{i\ell}$ due to the presence of the square root in each total relative velocity deficit term. By removing the square roots, the following expression is obtained:

$$\tilde{U} = \overbrace{\sum_{i=1}^{N}\sum_{j,k} w_{jk} u_{\infty}^{k} \xi_i}^{\text{Total inflow wind speed}} - \overbrace{\sum_{i=1}^{N}\sum_{\ell=1}^{N}\sum_{j,k} w_{jk} u_{\infty}^{k} (\delta_{i\ell}(\theta^j, u_{\infty}^k))^2 z_{i\ell}}^{\text{Total wind speed deficit proxy}} \tag{20}$$

the arguments of the square roots in Eq. (19) define a function closely related to the full root-squared expression. This linearization approach is similar to (Turner et al., 2014). Let the pre-processed coefficient in front of of $z_{i\ell}$ be

$$b_{i\ell} = \sum_{j,k} w_{jk} u_{\infty}^{k} (\delta_{i\ell}(\theta^j, u_{\infty}^k))^2 \tag{21}$$

combining Eq. (20) and Eq. (21) results in

$$\tilde{U} = \overbrace{\sum_{i=1}^{N}\sum_{j,k} w_{jk} u_{\infty}^{k} \xi_i}^{\text{Total inflow wind speed}} - \overbrace{\sum_{i=1}^{N}\sum_{\ell>i}^{N}(b_{i\ell} + b_{\ell i}) z_{i\ell}}^{\text{Total wind speed deficit proxy}} \tag{22}$$

which defines the objective function of the power-curve-free model. In comparison to the objective function in Eq. (18a), no power curve or continuous state variables are required.

Nonetheless, the presence of variables $z_{i\ell}$ can be troublesome. For the complete model, in addition to having these variables of combinatorial nature, constraints of the same kind must be incorporated: $z_{ij} \geq \xi_i + \xi_j - 1$, $z_{ij} - \xi_i$, $z_{ij} - \xi_j$. Experimental results show the heavy computational burden incurred when solving this formulation, impacting the ability of solving large-scale problems (Fischetti et al., 2016). To circumvent this, a big-M trick is incorporated (Wolsey, 2020), resulting in an exactly equivalent model, as reflected in formulation of Eq. (23).

The new objective function in Eq. (23a) modifies the component linked to the total wind speed deficit proxy by creating variables τ_i; this variable means total wind speed deficit proxy for WT in candidate location i. Equation (23b) defines τ_i, if a WT candidate location is inactive $\xi_i = 0$, then there is no deficit at this location, therefore $\tau_i = 0$, because of $M_i = \sum_{\ell=1:i\neq\ell}^{N} b_{i\ell}$, and the minimization nature of the problem for wind speed deficits. Oppositely, if $\xi_i = 1$, then τ_i is forced to be equal to $\sum_{\ell=1:i\neq\ell}^{N} \xi_\ell b_{i\ell}$. The next two equations are the same with those already presented in Sect. 3.1 for number of active WTs, and

minimum distance constraints. Finally, Eq. (23e) defines the domain of the required variables.

$$\text{maximize}_{\xi,\tau} \overbrace{\sum_{i=1}^{N}\sum_{j,k} w_{jk}u_\infty^k\xi_i}^{\text{Total inflow wind speed}} - \overbrace{\sum_{i=1}^{N}\tau_i}^{\text{Total wind speed deficit proxy}} \tag{23a}$$

$$\text{subject to: } \tau_i \geq \sum_{\ell=1:i\neq\ell}^{N} \xi_\ell b_{i\ell} + (\xi_i - 1)M_i \qquad \forall\, i \tag{23b}$$

$$n^{\min} \leq \sum_{i=1}^{N}\xi_i \leq n^{\max} \tag{23c}$$

$$\xi_i + \xi_q \leq 1 \qquad \forall\, i, q \in \boldsymbol{N}_i \tag{23d}$$

$$\xi \in \{0,1\} \quad \tau \in \mathbb{R}: \tau \geq 0 \tag{23e}$$

note that for the classic problem definition $n^{\min} = n^{\max} = n_{\mathrm{T}}$, the first part of the objective function becomes

$$\sum_{i=1}^{N}\sum_{j,k} w_{jk}u_\infty^k\xi_i = \sum_{j,k} w_{jk}u_\infty^k \sum_{i=1}^{N}\xi_i = \sum_{j,k} w_{jk}u_\infty^k n_{\mathrm{T}} = \text{constant}$$

for this situation, the objective function is thus equivalent to

$$\text{minimize}_{\xi,\tau} \sum_{i=1}^{N}\tau_i \tag{24}$$

this proxy objective function is very useful for formulating the program in the MILP category. While the work in (LoCascio et al., 2022) focuses on a different formulation (likely more accurate analytically than the one presented here) that is non-linear but gradient friendly, hence useful for continuous gradient-based optimization.

Compared to (Turner et al., 2014), the MILP program (23) with objective replaced by Eq. (24), linearizes the complexity of its largest set of constraints and variables from N^2 to N (Eq. (23b) and Eq. (23e)). Furthermore, the constraints in Eq. (23d), which can lead to infeasible points, are not neglected as in (Turner et al., 2014).

4 Neighborhood Search Heuristic

For addressing large-scale problems, a heuristic wrapping the MILP formulations given in Sect. 3 is introduced. It is based on neighborhood search and local branching theory (Fischetti and Lodi, 2003). The algorithm solves a sequence of MILPs, with different candidates number N and/or neighborhood search size K, taking advantage of robust and efficient implementations of branch-and-cut methods for MILP. The heuristic relies on the observation that for a fixed layout described by $\xi \in \{0,1\}^N$, the other state variables are straight forward to determine. This observation is valid for all problem formulations presented in Sect. 3. Given $\xi \in \{0,1\}^N$, for the power-curve-based model, the continuous state variables u can be determined through classical wake analysis, and the binary state variables η are directly determined by inspection of the velocities. Similarly, for

the power-curve-free model, the τ variables are trivially computed. The pseudo code of the Neighborhood Search Heuristic (NSH) is described in detail in Algorithm 1.

Algorithm 1 Neighborhood Search Heuristic (NSH) Algorithm

1: $\boldsymbol{C} \leftarrow \{N_1, \cdots, N_C\}, N \in \boldsymbol{C}$ {**Input candidates set**}

2: $\boldsymbol{T} \leftarrow \{T_1, \cdots, T_C\}, T \in \boldsymbol{T}$ {**Input times set**}

3: $\boldsymbol{V} \leftarrow \{K_1, \cdots, K_V\}, K \in \boldsymbol{V}$ {**Input neighborhood sizes set**}

4: *countern* $\leftarrow 1$ *counterv* $\leftarrow 1$

5: *Obtain initial incumbent of activation binary variables for WTs ξ with objective value o_b*

6: **for** $(\kappa = 1 : 1 : \kappa_{max})$ **do**

7:      $N \leftarrow \boldsymbol{C}[countern]$ $T \leftarrow \boldsymbol{T}[countern]$ $K \leftarrow \boldsymbol{V}[counterv]$

8:      *Formulate optimization model with N candidates (including the incumbent), either from Sect. 3.1 or Sect. 3.2*

9:      *Add Hamming distance constraint centered around the incumbent ξ, $\sum_{i:\xi_i=0} \xi_i + \sum_{i:\xi_i=1}(1-\xi_i) \leq K$*

10:      *Solve opt. model from algorithm lines (8) to (9) until optimality or computing time T with ξ as warm-starter*

11:      *Get the solution pool $\mathbf{S}$, where $\hat{\xi} \in \mathbf{S}$ represents the activation binary variables for WTs of an individual solution*

12:      *Apply **true objective function** over each solution $\hat{\xi} \in \mathbf{S}$, and obtain objective values set $\boldsymbol{O}$*

13:      *Compute $o_t \leftarrow \max \boldsymbol{O}$, and $i_t \leftarrow \arg\max \boldsymbol{O}$*

14:      **if** $o_t > o_b$ **then**

15:          $o_b \leftarrow o_t$

16:          $\xi \leftarrow \mathbf{S}[i_t]$

17:      **else**

18:          *counterv* $\leftarrow$ *counterv* $+1$

19:      **end if**

20:      **if** *counterv* $= |\boldsymbol{V}| + 1$ **then**

21:          *counterv* $\leftarrow 1$ *countern* $\leftarrow$ *countern* $+1$

22:      **end if**

23:      **if** *countern* $= |\boldsymbol{C}| + 1$ **then**

24:          *Break*

25:      **end if**

26: **end for**

---

285   The first three lines are the main inputs of the algorithm: the candidates set $\boldsymbol{C}$, the times set $\boldsymbol{T}$, and neighborhood sizes set $\boldsymbol{V}$. The first set contains the sizes N of the meshes to be considered, the second one is the maximum computing time T for the MILP solver for each size N and the last one is for the search size defined as the maximum number of changes K allowed to the incumbent solution. If the incumbent is improved, then the candidates set C, and neighborhood size K are kept, otherwise at least one of them is increased. The first step (line 5) is to obtain an initial incumbent binary variables, with the

set ξ storing the acquired value (0 or 1) for each variable $\xi_i : i \leq N$. The incumbent has an objective value of o_b calculated after the ***true objective function***. The true objective function refers to the real equation that represents the ultimate aim to be optimized. For example, if this is the AEP, then it is the product of the power calculation process, applying the considered wake and superposition models and the original power curve, and not the objective function of the implemented formulation, as in Eq. (18a), which is always an approximation.

The next step is to start the iterative process in line 6. Values for N, T, and K are fetched in line 7, followed by the formulation of the MILP model for candidates N accounting for the points of ξ. The Hamming distance, see e.g. (Fischetti and Lodi, 2003), centered around the incumbent point ξ, is added to the optimization model in line 9; this constraint reduces the search space as the number of changes of ξ are limited to K. The complete model is sent to the MILP solver with ξ as warm-starter, stopped when reaches either optimality or the assigned maximum computing time T.

After solver termination, the solution pool $\mathbf{S}$ is retrieved in line 11. The solution pool contains all the feasible layouts obtained in an iteration κ from the MILP solver. These points are a result of a linear programming relaxation or from applying heuristics in a given node, such as, relaxation induced search, polishing, and feasibility pump (IBM, 2022). It is very important to emphasize the aim of getting the whole pool instead of the best solution. This is done because of the imperfect correspondence between the true objective function and the objective function of the applied MILP model. For example, a solution which may have worse objective value, may actually have a better AEP based on the real model. One of the advantages of the NSH compared to the DEBO algorithm (Thomas et al., 2022c) is the reduced number of AEP evaluations. In an iteration κ, only $|\mathbf{S}|$ evaluations are required. Likewise, many of the other expensive calculations are done in a pre-processing stage. The whole pool of solutions is examined, and the best solution indexed by i_t with AEP of o_t is obtained in line 13. If o_t is actually greater than o_b, then the whole algorithm is re-centered around the new ξ (lines 14 to 16) and in the next iteration κ, the same values of N and K are maintained. Otherwise, the next value of K is taken (line 18), unless the set has been exhausted. In this case, the next candidates size N is considered given by $countern$, restarting the neighborhood set counter $counterv$ to one (lines 20 to 22). The NSH algorithm is terminated when all candidates set C have been processed (line 23 to 25). Another difference between the NSH and the DEBO is that the latter only changes the position of a single WT in a given iteration, while the former considers simultaneous modifications of several WT positions.

5 Computational Experiments

For a transparent benchmark of the proposed methods, the open access case studies from the IEA Wind Task 37 (Baker et al., 2019) are used for comparison. The Task 37 cases consider circular project areas with three different radius (1300 m, 2000 m, and 3000 m) and number of WTs (16, 36, and 64), n_T. Thus, Case I has a radius of 1300 m and $n_T = 16$ WTs, whereas Case II has radius 2000 m and $n_T = 36$, and Case III has radius 3000 m and $n_T = 64$, correspondingly.

The results of the statistical correlation between the proxy function given by the argument in Eq. (24) and AEP of the problem definition (Baker et al., 2019) are presented in Sect. 5.1 for each case. The performance of the proposed models in the case studies are shown in Sects. 5.2 (Case I), 5.3 (Case II), 5.4 (Case III). The power-curve-free model of Eq. (23) is

implemented with the Eq. (24) as objective function in these three sections. The true objective function in the NSH Algorithm 1 for these cases is the AEP of the problem definition. In the end, to prove the capabilities of power-curve-based model of Eq. (18), Sect. 5.5 displays results after applying this formulation with a modified objective function to express a metric similar to NPV.

The main parameters of the wake model in Sect. 2.1 are fixed to $C_\mathrm{T} = 8/9$ and $k_\mathrm{y} = 0.0324555$, according to (Baker et al., 2019). Wind resource is modelled using a wind rose approach where the wind resource is binned in J directions, and for a specific direction j (θ^j), wind speeds are discretized in Υ sectors. For the case studies, the wind rose is composed of 16 directions and a single wind speed k of 9.8 ms^{-1}, shown in Fig. 2. The power curve from Eq. (8) modelling the IEA37 3.35 MW reference turbine (with diameter of $D = 130$ m) is used in the case studies, ensuring replicability of results (IEA Wind Task 37, 2019; Baker et al., 2019). The main parameters are $p^\mathrm{rated} = 3.35$ MW, $u^\mathrm{rated} = 9.8$ ms^{-1}, $u^\text{cut-in} = 4$ ms^{-1}, and $u^\text{cut-out} = 25$ ms^{-1}, and is plotted in Fig. 1. The parameter d^min is set to $2D$.
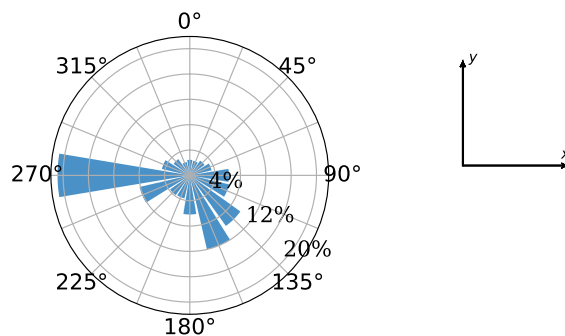
Figure 2. Wind rose used in the computational experiments. Taken from open access source (IEA Wind Task 37, 2019).

The experiments in Sects. 5.2, 5.3, and 5.4 have been carried out on an Intel Core i7-6600U CPU running at 2.80 GHz with four logical processors and 16 GB of RAM. For the experiment in Sect. 5.5, a larger resource is used, an Intel Xeon Gold 6226R CPU running at 2.90 GHz with 32 virtual cores and 640 GB of RAM.

The selected MILP solver is the commercial branch-and-cut algorithm implemented in IBM ILOG CPLEX Optimization Studio V20.1 (IBM, 2022). Apart from the number of threads and time limit settings, a few other parameters are also set to differently than default values. One is the parameter returning high-quality feasible solutions early in the process, for which, the (CPX_MIPEMPHASIS_HEURISTIC) is activated. The intention is to generate more feasible layouts which is important for the neighborhood search algorithm. Additionally, strong branching is used for variable selection given the large size of the models (CPX_VARSEL_STRONG is selected). The intention is to reduce the size of the search tree and thus the memory requirements compared to default settings.

The number N and positions $\mathbf{p}_i$ for $i \leq N$ of the candidate locations are of course very important parameters for the discrete modelling techniques. A customized automatic strategy based on independently sampling the boundary and interior area of the

circular domain **F** has been employed. An example of the sampling strategy for these particular case studies giving $N = 467$ is illustrated in Fig. 3.
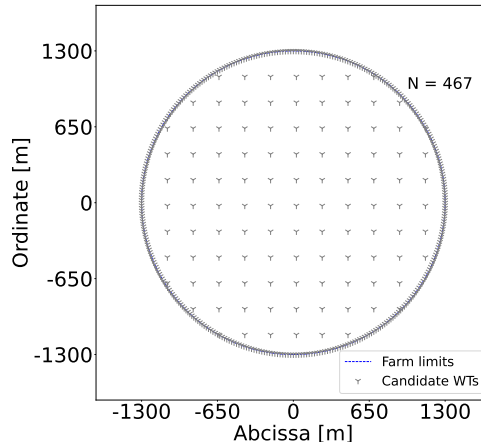
Figure 3. Example of generation of WTs candidate locations N.

The boundary is densely sampled, as a candidate point is defined every natural angle from $0°$ to $359°$, i.e. 360 candidate points are provided since it is intuitively expected that a good portion of the WTs will be placed in the boundaries to decrease wake losses. For the interior, a set of finite parallel line segments are generated and the candidates points are then taken along those segments. In the example of Fig. 3, the slope of the line segments is zero, and the distance between points and lines is equal to $1.7D$.

5.1 Correlations

To validate the approach modelled by the MILP formulation of Eq. (23) (i.e. the power-curve-free model), 5000 random feasible WT layouts are created. For each of them, the AEP (Baker et al., 2019), the total theoretical wind speed, U, given by Eq. (19), the total wind speed proxy, $\tilde{U}$, defined by Eq. (22), and total wind speed deficit proxy, $\sum_{i=1}^{N} \tau_i$, argument of Eq. (24), are calculated. Although the random way of generating the layouts is biased towards high-quality solutions, the interest is in the general trend and can be assumed to be fairly representative for the whole domain.

In all cases Pearson product-moment linear correlation coefficients (Pearson, 1895) are used to extract information from the data and collected in Table 1 for all pairs. This coefficient illustrates the degree to which the movement of pairs of variables is associated in a linear fashion. The correlation plots of Fig. 4 present the graphical representation of the relations for Case I.

The correlation between AEP and the total theoretical wind speed is shown in Fig. 4a for the Case I. The main observation is the very strong linear relation between these two variables as illustrated by the correlation coefficient of 0.97. Interestingly, this reflects the rather low influence of the WT power curve in obtaining high-quality feasible points. The relation between U and $\tilde{U}$ is represented in Fig. 4b, resulting in an almost identical linear connection between them, as in the previous graph. When one looks into AEP vs $\sum_{i=1}^{N} \tau_i$, however, it is noticeable that the Pearson coefficient decreases to -0.88. There is a wider area

in the body of points that causes this behaviour. Note that in contrast to the previous two figures, there is a negative correlation because the comparison is done in terms of wind speed deficit instead of total wind speed. In spite of this deterioration, the linear correlation is still considered quite strong. These results motivate the approach where the minimization of a proxy total wind speed deficit can lead to high-quality AEP solutions. The NSH Algorithm 1 helps correcting the imperfect correspondence between these two variables during the optimization routine as reflected in Sect. 4.

Table 1. Pearson product-moment linear correlation coefficients for all case studies.

Case	AEP vs Theoretical wind speed	Theoretical vs Proxy wind speed	AEP vs Proxy wind speed deficit
Case I	0.97	0.96	-0.88
Case II	0.97	0.95	-0.85
Case III	0.96	0.88	-0.72

(a) Correlation between AEP and the theoretical wind speed.

(b) Correlation between the theoretical and approximated wind speeds.

(c) Correlation between AEP and the approximated wind speed deficit.
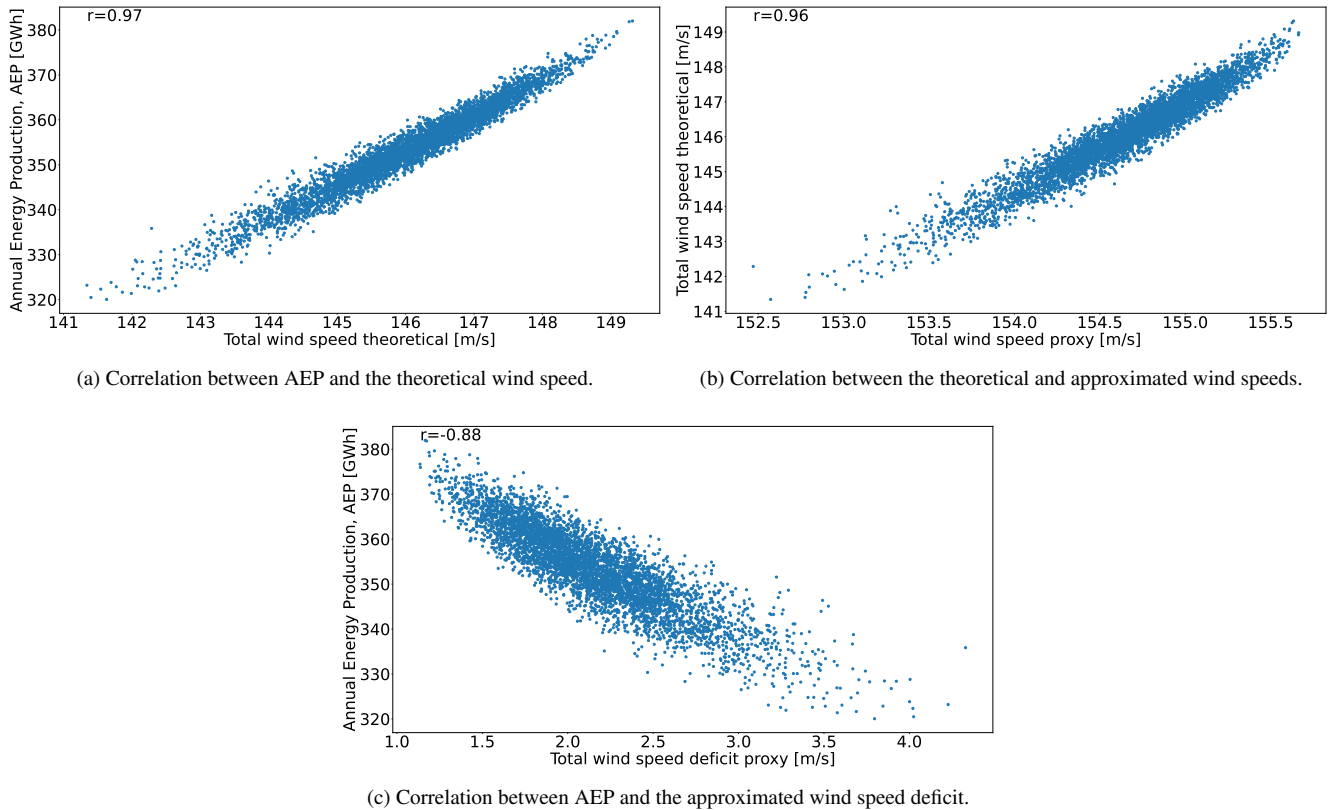
Figure 4. Correlation plots for 5000 randomly generated wind turbine layouts for Case I.

The general trends of the correlation plots for Case II are very similar. Correlations between AEP versus theoretical total wind speed (0.97), and theoretical total wind speed versus total wind speed proxy (0.95) are still very strong. Nonetheless,

there is a slight decrease between AEP vs total wind speed proxy (down to -0.85 from -0.88 previously), as the spread for middle velocity values is larger. The linear relation is deemed as satisfactory enough to carry on with the application of model of Eq. (23) with objective function Eq. (24).

The very strong linear relation between AEP and the theoretical total wind speed (0.96) is observed also for Case III, prompting to a very interesting conclusion. Although almost all research in the WFLO space focuses strictly on power modelling (which brings a great deal of complexity due to the non-linear and non-differentiable properties of WT power curve), using an exact model for determining total wind speed as objective function alleviates the computational complexity, while finding high-quality solutions in terms of AEP. However, one should note that deterioration in the correlation still exists, potentially leading to lower quality results.

Likewise, correlations stemming from the proxy to calculate total wind speed deficit are lowered in Case III. This is the case for both with the total wind speed theoretical (0.88) and the AEP (-0.72). Keep in mind that the reason to formulate such approximation is to fit in the context of integer programming to leverage theory and state-of-the-art algorithms of this mature field. However, the price to pay is to lose fidelity to represent the real (true) target to optimize. The deterioration in the correlation of these pairs of variables may also suggest the need to resort to the power-curve-based model for some applications. Whether the price is too high or not is reflected in the reachable solution quality. Sects. 5.2, 5.3, and 5.4 present the optimization results for the cases of fixed number of WTs that will ultimately help to elaborate a final evaluation regarding the adopted modelling technique.

5.2 Case I: 16 WTs

The evolution of two of the proposed optimization frameworks is given in Fig. 5 (clock time given in the abscissa). The green line of the full model is obtained after solving the model of Eq. (23) with objective function as in Eq. (24) for $N = 1014$ without implementing the NSH. It represents the incumbent solution in terms of AEP (not total wind speed deficit proxy) obtained by post-processing the CPLEX's log. The blue line results after applying the NSH with the model of Eq. (23) plus objective Eq. (24), and AEP as true objective function in Algorithm 1. The main inputs are $C = \{467, 590, 1014\}$ (set of candidate locations), $T = \{1, 1.5, 2\}$ h (set of max computing times for each candidate location), $V = \{2, 4, 6, 16\}$ (set of neighborhood search sizes). See Sect. 4. These inputs are tuned after evaluating the performance of the method using different values. In general, the first two elements of C consists of moderately big values, relatively close to each other, while the last element is sizeably greater in the search of the best possible solution. Each element $N \in C$ has associated a computing time T. Finally, the first elements of V are relatively low values to favour termination of the solver due to optimality, and then they start increasing to refine the search. The red line is for establishing a reference of AEP value, this comes from the best performing method in the survey of IEA Wind Task 37 (Baker et al., 2019), the SNOPT plus Wake Expansion Continuity (WEC) (Thomas and Ning, 2018; Thomas et al., 2022b). Time evolution for the SNOPT+WEC is not reflected in this graph, as this information is unavailable. Results for the benchmark against a testbed of different algorithms are available in Table 3.

The NSH computing time results in Fig. 5 do not reflect the instant where the incumbent is found, but the time progress of this algorithm, which is dependent on the execution of the MILP solver at each iteration. Table 2 contains information about the

17

values of N, K, T, and termination criterion of the solver after each iteration κ of the NSH Algorithm 1 (beginning from point 2 where $\kappa = 1$). This means that, in iterations where the termination criterion is time (and not optimality), one could fine-tune

410   T for an earlier stop, shortening the total time. This is particularly more relevant in cases where internal heuristics of the solver are activated at the root node of the search tree, coming up with the largest portion of solutions very early in the process. Consequently, the total computing time, for all cases, is conservative and should be taken as an approximated reference.

    The initial layout (point 1), labelled in Fig. 6a, is set up by arbitrarily by picking up candidate locations around the circular boundary; this layout has an AEP of 387 GWh. From now on, the presented percentages are calculated with respect to the last

415   commented AEP improvement. Between points 2 to 7 where $N = 467$ and $K = 2$, the models are solved to optimality (gap of 0%), and the solution is improved by 2.92% in only 56 s. After a short plateau, the solution is markedly refined by 2.96% from point 10 to 13 by performing a search of the domain with $K = 16$, and restarting the model every 1 h with a new warm-starting.
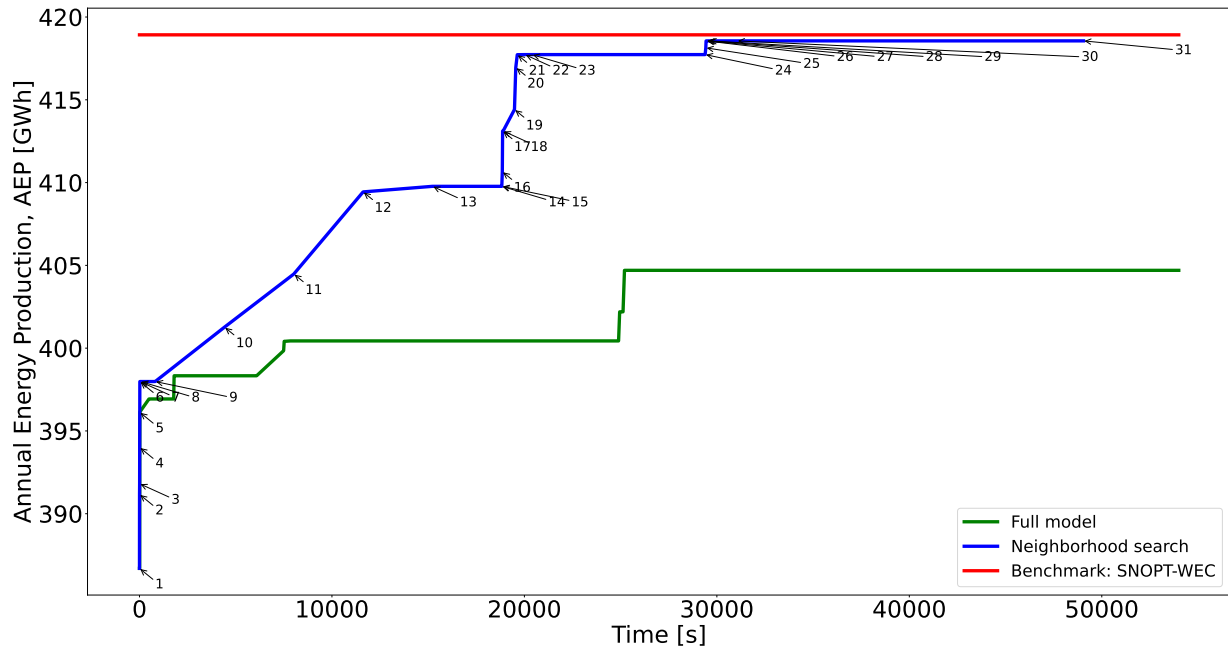
Figure 5. Performance of two different optimization approaches for Case I and comparison with existing best benchmark results.

    The next considerable jump happens for $N = 590$ and $2 \leq K \leq 6$ in around 20 min, elevating the AEP by 1.94%. After, again, a plateau without improvements, when N reaches its maximum value of 1014, the solution is maximized to the final

420   value of 418 GWh during the lowest values of K. For this particular instance, the greatest value of $K = 16$ is exploited for the lowest number of candidate points N, where the largest improvement comes up.

    The benefit of the proposed neighborhood search strategy is shown in Fig. 5. Solving the full model is significantly slower, leading actually to a worse solution (3.31% lower). The capacity of the NSH to iterate over different values of candidate points N and search sizes K brings alone not only improvements in terms of solution time and solution quality, but also less

425   computational resources as the RAM memory generally scales faster when solving the single model.

The initial and final solution layouts for this case study are illustrated in Fig. 6. The importance of finely sampling the boundaries of the available area is evident in Fig. 6b, because 7 out of the 16 WTs are placed in that subdomain.

Table 2. Information about the values of N, K, T, and ter mination criterion of the solver after each point in Fig. 5.

Point	K, N		Termination criterion	Point	K, N		Termination criterion
1	Initial point		-	17	$K=4$	$N=590$	opt. [0.24 min]
2	$K=2$	$N=467$	opt. [0.05 min]	18	$K=4$	$N=590$	opt. [0.46 min]
3	$K=2$	$N=467$	opt. [0.06 min]	19	$K=6$	$N=590$	opt. [9.79 min]
4	$K=2$	$N=467$	opt. [0.04 min]	20	$K=6$	$N=590$	opt. [1.10 min]
5	$K=2$	$N=467$	opt. [0.06 min]	21	$K=6$	$N=590$	opt. [1.29 min]
6	$K=2$	$N=467$	opt. [0.05 min]	22	$K=6$	$N=590$	opt. [6.64 min]
7	$K=2$	$N=467$	opt. [0.07 min]	23	$K=6$	$N=590$	opt. [6 min]
8	$K=4$	$N=467$	opt. [0.49 min]	24	$K=16$	$N=590$	1.5 h
9	$K=6$	$N=467$	opt. [12.69 min]	25	$K=2$	$N=1014$	opt. [0.53 min]
10	$K=16$	$N=467$	1 h	26	$K=2$	$N=1014$	opt. [0.20 min]
11	$K=16$	$N=467$	1 h	27	$K=2$	$N=1014$	opt. [0.20 min]
12	$K=16$	$N=467$	1 h	28	$K=4$	$N=1014$	opt. [0.95 min]
13	$K=16$	$N=467$	1 h	29	$K=4$	$N=1014$	opt. [1.10 min]
14	$K=16$	$N=467$	1 h	30	$K=6$	$N=1014$	opt. [24.37 min]
15	$K=2$	$N=590$	opt. [0.06 min]	31	$K=16$	$N=1014$	2 h
16	$K=4$	$N=590$	opt. [0.43 min]				

Finally, Table 3 compares the proposed method to a large number of different approaches from the IEA37 reference study (Baker et al., 2019). The results for all case studies are presented, where I, II, and III make reference to cases from this section, Sect. 5.3, and Sect. 5.4, respectively.

The third column of Table 3 reports the difference of the AEP with respect to the proposed method for the smallest case study. The resulting AEP is better than almost all the other alternatives, except to the SNOPT+WEC, where a nearly identical objective value is achieved. When directly comparing to to typical metaheuristics (genetic algorithm, particles swarm optimization, etc), that do not use explicit gradients information, the presented method seems to perform well, being able of determining a similar layout quality in less than 2 h, which is generally faster than average computing time of these kind of algorithms. In a broader context, beyond the presented numerical comparisons, discrete optimization approaches, as the MILP ones presented in this manuscript, could be formulated to cope with problem definitions with required functionalities that in theory continuous optimization methods can not support (or at least the implementation becomes strenuous).

Table 3. Results for all three benchmark cases from other algorithms (G, gradient-based and GF, gradient-free) obtained while allowing WT locations to vary continuously. Values reproduced from (Baker et al., 2019). The difference column shows how the proposed heuristic with the power-curve-free model performs in comparison. Negative percentages means that the proposed method performs better than the corresponding algorithm.

Method	AEP I [GWh]	Diff. I [%]	AEP II [GWh]	Diff. II [%]	AEP III [GWh]	Diff. III [%]
SNOPT+WEC (G)	418.92	0.09	863.68	-0.19	1513.31	0.85
fmincon (G)	414.14	-1.06	820.39	-5.19	1336.16	-10.95
SNOPT (G)	412.25	-1.51	846.36	-2.19	1476.69	-1.59
SNOPT (G)	411.18	-1.76	844.28	-2.43	1445.97	-3.64
Preconditioned SQP (G)	409.69	-2.12	849.37	-1.84	1506.39	0.39
Mul.interior-point (G)	408.36	-2.44	851.63	-1.58	1480.85	-1.31
Full pseudo-gradient (GF)	402.32	-3.88	828.75	-4.23	1455.08	-3.03
Basic genetic algorithm (GF)	392.59	-6.20	777.48	-10.15	1332.88	-11.17
Simple particle swarm (GF)	388.76	-7.12	776	-10.32	1364.94	-9.04
Simple pseudo-gradient (GF)	388.34	-7.22	813.54	-5.98	1422.27	-5.22
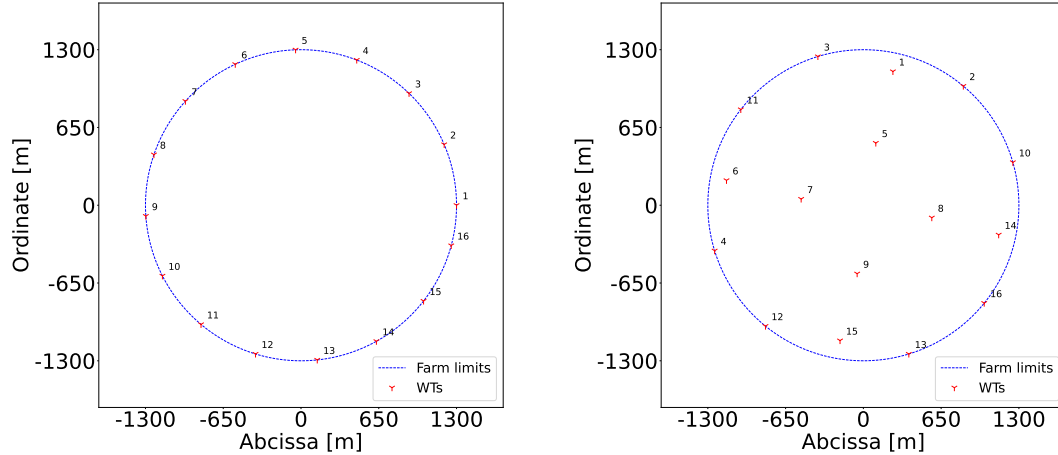
(a) Initial wind farm layout provided to the heuristic.

(b) Final wind farm layout obtained by the heuristic.

Figure 6. Generated wind farm layouts for the benchmark Case I with 16 turbines.

The power-curve-based model of Eq. (18) within the NSH using the same AEP formulation as true objective function, provides a solution 1.18% lower in objective value in around $36\,\mathrm{h}$ using the computer system with 32 virtual cores. Although the quality of the layout is very close to the one schematized in Fig. 6b, the larger computational resources favour implementing

the power-curve-free model for problems with fixed number of WTs. Therefore, Sects. 5.3 and 5.4 are present only the results reached after the application of the power-curve-free model embedded into the NSH.

5.3 Case II: 36 WTs

445 The evolution of the proposed methods, and the initial and final WT layouts are plotted in Fig. 7 and Fig. 8, respectively. Table 4 displays the data linked to each point of Fig. 7. Main inputs are $C = \{477, 684, 1907\}$, $T = \{1, 1.5, 2\}$ h, $V = \{2, 4, 8, 16, 36\}$. The blue line (model of Eq. (23) with objective function Eq. (24) plus NSH Algorithm 1) has clearly three sectors stemming from each value of $N \in C$. The initial WT layout (Fig. 8a) - also determined by choosing roughly equidistant candidate locations in the boundary - has an AEP of 796 GWh. As for Case I, improvement percentages are calculated using the last

450 commented step as the baseline. After seven NSH iterations (point 8) in 41 s, the incumbent is improved by 1.84%, when $N = 477$ and $2 \leq K \leq 4$, being able to solve each model instantiation to optimality.
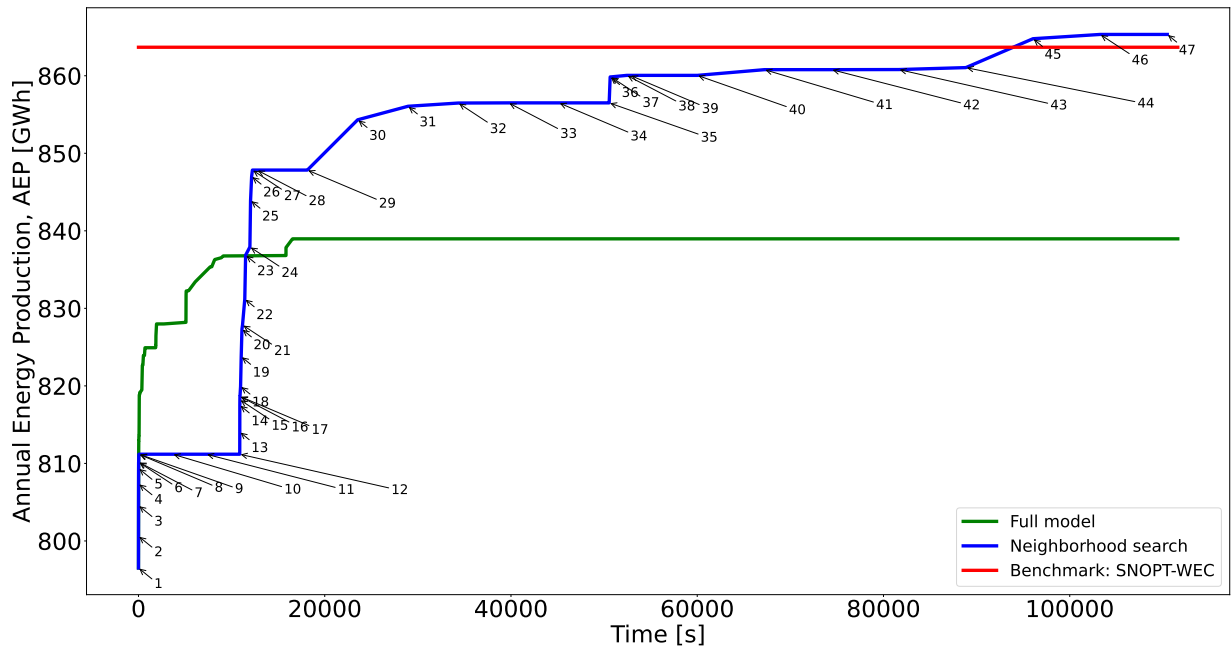
Figure 7. Performance of two different optimization approaches for Case II and comparison with existing best benchmark results.

After a three-hours-plateau linked to $8 \leq K \leq 36$ (four iterations), N is raised to 684, resulting in the largest AEP enhancement, as shown in Fig. 7. The energy production increases with 4.51% after only 23 min in point 27. This noticeable improvement comes after solving to optimality models with rather small neighborhood search sizes $2 \leq K \leq 4$. The conve-

455 nience of allowing large neighborhood search sizes as $K = 16$ or $K = 36$ is reflected from this moment. From point 30 to 33 (6 h) with $K = 16$ the incumbent is slowly boosted by nearly 1%. Again, after a three-hours-plateau, N becomes equal to 1907,

21

and in around $32 \min$ for $2 \leq K \leq 4$, the AEP is augmented by 0.41%. Then, the large neighborhood search starts for $K = 16$ and $K = 36$, and after a total of $16 \mathrm{h}$, the final solution of $865 \mathrm{GWh}$ (increment of 0.61%) is achieved (Fig. 8b).

Table 4. Information about the values of N, K, T, and ter mination criterion of the solver after each point in Fig. 7.

Point	K, N		Termination criterion	Point	K, N		Termination criterion
1	Initial point		-	25	$K = 4$	$N = 684$	opt. [1.15 min]
2	$K = 2$	$N = 477$	opt. [0.03 min]	26	$K = 4$	$N = 684$	opt. [1.90 min]
3	$K = 2$	$N = 477$	opt. [0.03 min]	27	$K = 4$	$N = 684$	opt. [1.38 min]
4	$K = 2$	$N = 477$	opt. [0.04 min]	28	$K = 4$	$N = 684$	opt. [8.31 min]
5	$K = 2$	$N = 477$	opt. [0.05 min]	29	$K = 8$	$N = 684$	1.5 h
6	$K = 2$	$N = 477$	opt. [0.05 min]	30	$K = 16$	$N = 684$	1.5 h
7	$K = 2$	$N = 477$	opt. [0.04 min]	31	$K = 16$	$N = 684$	1.5 h
8	$K = 4$	$N = 477$	opt. [0.37 min]	32	$K = 16$	$N = 684$	1.5 h
9	$K = 4$	$N = 477$	opt. [0.49 min]	33	$K = 16$	$N = 684$	1.5 h
10	$K = 8$	$N = 477$	1 h	34	$K = 16$	$N = 684$	1.5 h
11	$K = 16$	$N = 477$	1 h	35	$K = 36$	$N = 684$	1.5 h
12	$K = 36$	$N = 477$	1 h	36	$K = 2$	N=1907	opt. [1.65 min]
13	$K = 2$	$N = 684$	opt. [0.07 min]	37	$K = 2$	N=1907	opt. [1.12 min]
14	$K = 2$	$N = 684$	opt. [0.07 min]	38	$K = 4$	N=1907	opt. [28.40 min]
15	$K = 2$	$N = 684$	opt. [0.07 min]	39	$K = 4$	N=1907	opt. [5.97 min]
16	$K = 2$	$N = 684$	opt. [0.08 min]	40	$K = 8$	N=1907	2 h
17	$K = 2$	$N = 684$	opt. [0.09 min]	41	$K = 16$	N=1907	2 h
18	$K = 4$	$N = 684$	opt. [1 min]	42	$K = 16$	N=1907	2 h
19	$K = 4$	$N = 684$	opt. [1 min]	43	$K = 36$	N=1907	2 h
20	$K = 4$	$N = 684$	opt. [1.33 min]	44	$K = 36$	N=1907	2 h
21	$K = 4$	$N = 684$	opt. [0.98 min]	45	$K = 36$	N=1907	2 h
22	$K = 4$	$N = 684$	opt. [4.05 min]	46	$K = 36$	N=1907	2 h
23	$K = 4$	$N = 684$	opt. [1.47 min]	47	$K = 36$	N=1907	2 h
24	$K = 4$	$N = 684$	opt. [7.65 min]				

The full model (i.e. without implementing the NSH algorithm) initially provides better solutions within the first $3 \mathrm{h}$, but then lags behind in solution quality compared to the NSH algorithm in the long run (lower 3.05%), as shown in in Fig. 7.

For this case, the proposed method reaches the best solution, as shown in the fifth column of Table 3. The SNOPT+WEC is again the closest contender. When uniquely comparing to GF methods, the proposed method matches the best solution from

those algorithms in around 3 h, which is generally a reasonable computing time compared to methods where gradients are not explicitly utilized in the optimization process, especially to metaheuristics as genetic algorithm or swarm optimization.

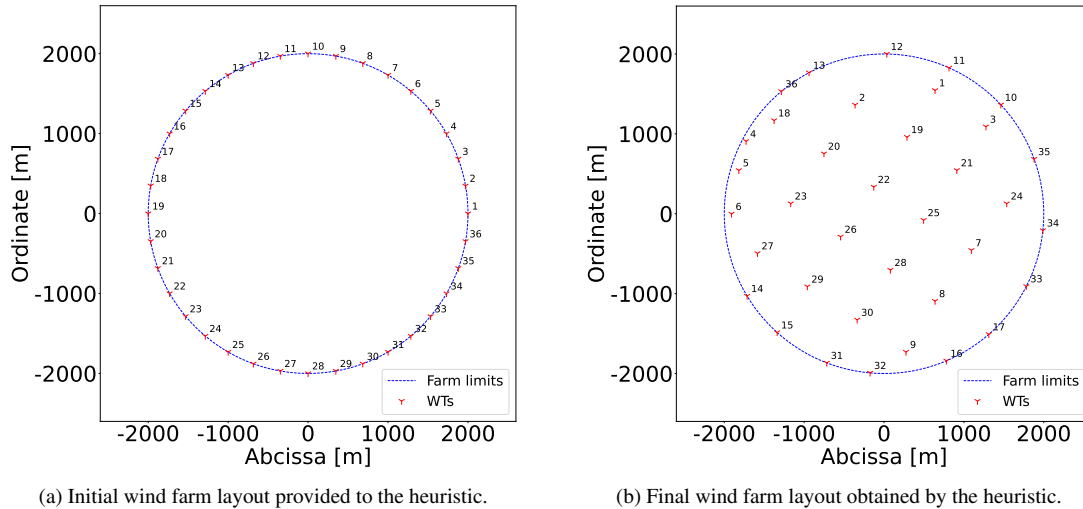(a) Initial wind farm layout provided to the heuristic.

(b) Final wind farm layout obtained by the heuristic.

Figure 8. Generated wind farm layouts for the benchmark Case II with 36 wind turbines.

5.4 Case III: 64 WTs

The evolution of the proposed methods, and the initial and final WT layouts are displayed in Fig. 9 and Fig. 10, respectively. Table 5 displays the data linked to each point of Fig. 9. Main inputs are $C = \{625, 1017, 2741\}$, $T = \{1, 1.5, 2\}$ h, $V = \{2, 4, 8, 16, 32, 64\}$. Note that in comparison the number of elements of V has been increased by one after each study case. This has been done taking into account the number of WTs. Likewise, the values of $N \in C$ are larger to cover for the wider project areas.

Comparing blue lines of Fig. 5, Fig. 7, and Fig. 9 is evident that for the last case the curve shows less sudden increases. The largest change occurs after 27 s where the initial solution (Fig. 10a) with AEP of 1395 GWh is improved by 3.18% for $N = 625$ and $K = 2$ up to point 9, reaching optimality in few seconds. With $4 \leq K \leq 8$ the model instantiations are solved to optimality in minutes, obtaining a solution improved by 0.18%.

After point 13 one notes a plateau without improvement for $N = 625$ and $K \geq 16$, i.e. a large neighborhood search does not lead to further enhancements. Due to this, N is enlarged to 1017, where the second largest boost (increase of 2.12%) comes, with the largest search size ($K = 64$) resulting in the best improvement. This enhancement occurs after 13 h of starting the NSH (point 26). From point 28, $N = 2741$ and for $2 \leq K \leq 4$ the solver reaches optimality; slowly converging to the final solution of 1500 GWh (Fig. 10b).

Seventh column of Table 3 shows that the SNOPT+WEC and the preconditioned SQP provide slightly better layouts than the proposed method. However, the algorithm provides feasible layouts that improve the objective compared to all the gradient-free approaches.
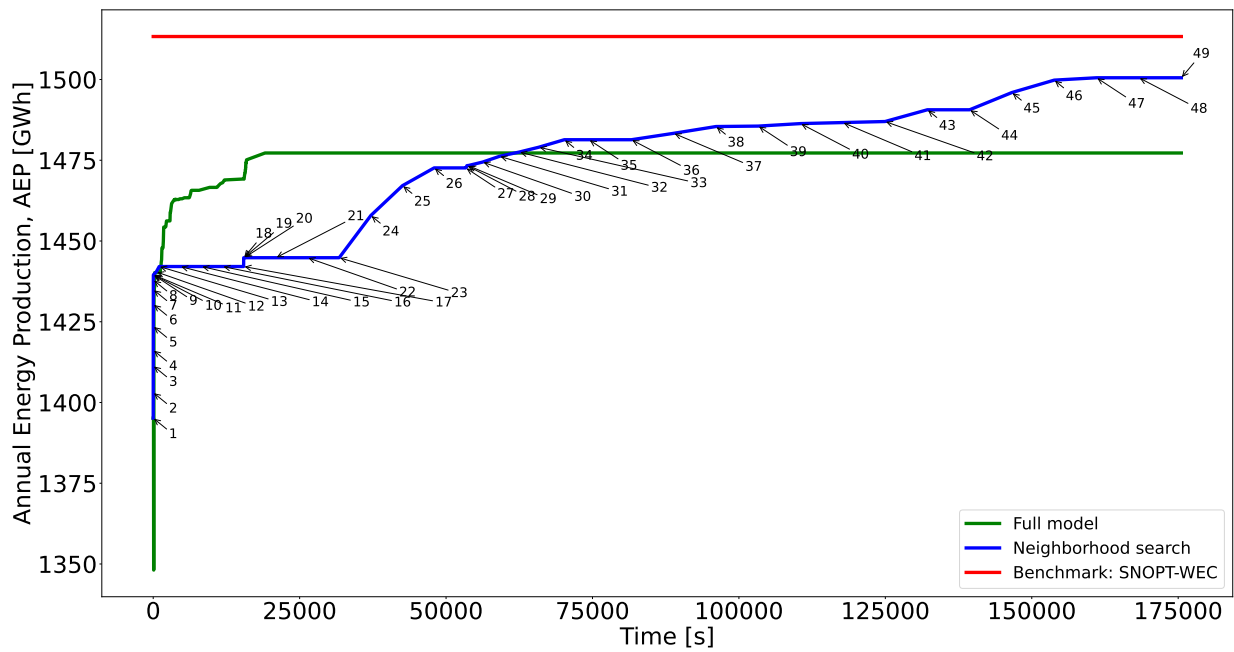
Figure 9. Performance of two different optimization approaches for Case III and comparison with existing best benchmark results.
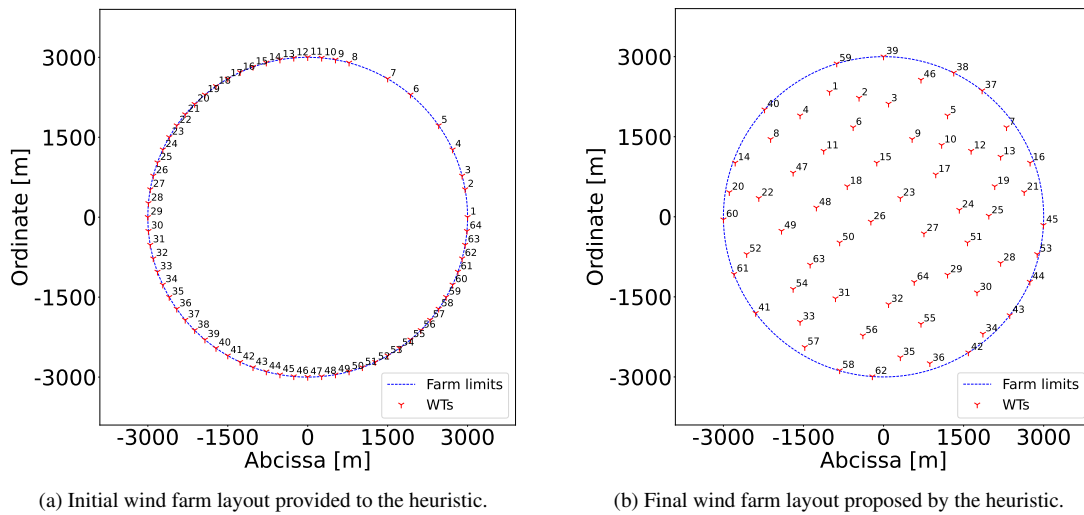

(a) Initial wind farm layout provided to the heuristic.

(b) Final wind farm layout proposed by the heuristic.

Figure 10. Generated wind farm layouts for benchmark Case III with 64 wind turbines.

Table 5. Information about the values of N, K, T, and ter mination criterion of the solver after each point in Fig. 9.

Point	K, N		Termination criterion	Point	K, N		Termination criterion
1	Initial point			26	$K = 64$	$N = 1017$	1.5 h
2	$K = 2$	$N = 625$	opt. [0.03 min]	27	$K = 64$	$N = 1017$	1.5 h
3	$K = 2$	$N = 625$	opt. [0.03 min]	28	$K = 2$	$N = 2741$	opt. [3.22 min]
4	$K = 2$	$N = 625$	opt. [0.03 min]	29	$K = 2$	$N = 2741$	opt. [2.93 min]
5	$K = 2$	$N = 625$	opt. [0.04 min]	30	$K = 4$	$N = 2741$	opt. [40.82 min]
6	$K = 2$	$N = 625$	opt. [0.05 min]	31	$K = 4$	$N = 2741$	opt. [47.99 min]
7	$K = 2$	$N = 625$	opt. [0.04 min]	32	$K = 4$	$N = 2741$	opt. [55.95 min]
8	$K = 2$	$N = 625$	opt. [0.04 min]	33	$K = 4$	$N = 2741$	opt. [54.74 min]
9	$K = 2$	$N = 625$	opt. [0.05 min]	34	$K = 4$	$N = 2741$	opt. [72.46 min]
10	$K = 2$	$N = 625$	opt. [0.04 min]	35	$K = 4$	$N = 2741$	opt. [69.85 min]
11	$K = 4$	$N = 625$	opt. [0.33 min]	36	$K = 8$	$N = 2741$	2 h
12	$K = 8$	$N = 625$	opt. [7.92 min]	37	$K = 16$	$N = 2741$	2 h
13	$K = 8$	$N = 625$	opt. [8.31 min]	38	$K = 16$	$N = 2741$	2 h
14	$K = 8$	$N = 625$	1 h	39	$K = 16$	$N = 2741$	2 h
15	$K = 16$	$N = 625$	1 h	40	$K = 16$	$N = 2741$	2 h
16	$K = 32$	$N = 625$	1 h	41	$K = 16$	$N = 2741$	2 h
17	$K = 64$	$N = 625$	1 h	42	$K = 16$	$N = 2741$	2 h
18	$K = 2$	$N = 1017$	opt. [0.17 min]	43	$K = 16$	$N = 2741$	2 h
19	$K = 2$	$N = 1017$	opt. [0.26 min]	44	$K = 16$	$N = 2741$	2 h
20	$K = 4$	$N = 1017$	opt. [1.35 min]	45	$K = 32$	$N = 2741$	2 h
21	$K = 8$	$N = 1017$	1.5 h	46	$K = 32$	$N = 2741$	2 h
22	$K = 16$	$N = 1017$	1.5 h	47	$K = 32$	$N = 2741$	2 h
23	$K = 32$	$N = 1017$	1.5 h	48	$K = 32$	$N = 2741$	2 h
24	$K = 64$	$N = 1017$	1.5 h	49	$K = 64$	$N = 2741$	2 h
25	$K = 64$	$N = 1017$	1.5 h				

5.5 Case IV: 10-50 WTs

Although in most projects today the total capacity for grid connection is decided already in the early planning phases, in the future one can envisage situations where flexibility in optimizing the number of wind turbines in a project would yield benefits.

Even if the power-curve-free model (Sect. 3.2) exhibits a quite good performance in terms of AEP and computing time for fixed number of WTs (when AEP and NPV are basically the same metric), it is not very well suited when variable number

of wind turbines are considered. Based on computational experiments not included in the paper, the power-curve-free model embedded in the NSH terminates too early in the search process, resulting in a worse solution than the alternative discussed in the following.

For such an optimization, the power-curve-based mathematical program of Sect. 3.1 may be handy as the number of generators is allowed to vary between a lower and upper bound, $n^{\min}$ and $n^{\max}$, respectively. For illustration, a domain defined by a circle with radius 1300 m, and variable number of WTs between 10 and 50 are utilized. These parameters are set relatively arbitrarily but with sufficient distance to reasonably expect that the limits are not reached. The aim is to illustrate the ability of the method in reaching non-trivial solutions, resulting in a an optimized design with an intermediate number of wind turbines.

Keep in mind that for this case, a linear superposition model for the AEP component in the NPV calculation is considered. In this sense, the original WT power curve as depicted in Fig. 1 is used. NPV is the true objective function when applying the NSH Algorithm 1. The modified objective function of MILP model of Eq. (18) for this case has the form (Cogency, 2014):

$$\underset{\xi, \eta, u}{\text{maximize}} \; - \sum_{i=1}^{N} c_{\text{wt}} \xi_i + 8760 \sum_{y=1}^{Y} \sum_{i=1}^{N} \sum_{j,k} \sum_{l=1}^{m+2} \frac{c_{\text{e}} w_{jk} \eta_{ijk}^{l} p(u_{\text{m}}^{l})}{(1+r)^y} \tag{25}$$

where c_{wt} is the cost per WT in mEUR, c_{e} the energy price in mEURMWh^{-1}, r is the discount rate in %, and Y is the number of years of lifetime of the project. For this case study, values of $c_{\text{wt}} = 6.7$ mEUR (Mishnaevsky Jr and Thomsen, 2020), $c_{\text{e}} = 0.00015$ mEURMWh^{-1} (Nord Pool, 2022), $r = 5\%$, and $Y = 20$ are assumed. The general form of the NPV equation (Cogency, 2014) is defined by the sum of the present value of cash flows (Discounted Cash Flow, DCF) of a project under analysis. In Eq. (25), the first sum is a negative cash flow representing purchase of the WTs at the construction stage of the project, while the next term represents positive cash flows coming from trading the electricity in the market. Because of the additive nature of the NPV metric and since the focus is on evaluating investment vs revenues, by maximizing Eq. (25), a fully comprehensive NPV metric is equivalently improved.

The model of Eq. (18) with modified objective function Eq. (25), embedded in the NSH Algorithm 1 with NPV as target function is executed in three runs. For the first run the number of turbines is fixed to $n^{\min} = n^{\max} = 10$, while for the second the number of turbines remains fixed but is increased to $n^{\min} = n^{\max} = 50$. For the third run the number of wind turbines is allowed to vary between $n^{\min} = 10$ and $n^{\max} = 50$. The Algorithm 1 input parameters are $\boldsymbol{C} = \{467, 590, 1014\}$, $\boldsymbol{T} = \{1, 1.5, 2\}$ h, $\boldsymbol{V} = \{2, 4, 6, 8, 24\}$. The results are plotted in Figure 11.

When the number of turbines is fixed to 10, the NPV evolution (green line in Fig. 11b) is driven by the AEP (green line in Fig. 11a). Both curves are monotonically increasing, reaching a final value of NPV of $= 456.40$ mEUR. The same behaviour is visible for $n_{\text{T}} = 50$, although the final NPV is greater (683.53 mEUR), see blue line Figure 11b. In the second study, the positive difference in DCF from the revenues surpasses the associated extra investment costs from the additional 40 wind turbines considered. The significant increase in the number of WTs doubles the computing time, due to the large increase in the number of variables, selecting 50 WTs entails significantly more possible combinations of valid solutions.

An interesting question is whether there is a larger NPV in between the bounds of WT number. For the optimization program with variable number of WTs, the evolution of the WTs number in Fig. 11c and the AEP in Fig. 11a (see black lines in these figures) exhibits a perfect correspondence. The more WTs the larger AEP, in spite of the increased wake losses. The curves

increase in time, up to a point where the model estimates that further increase of WTs would not lead to a better NPV. The final number of WTs is 34. The NPV evolution in Fig. 11b (black line) naturally only improves with time, resulting in a final value of 795.86 mEUR. Note that the NPV in this case is greater than when a larger number of WTs (i.e. 50) was considered and

525 of course when only 10 were considered. Interestingly, the optimization program with 50 fixed number of WTs finds a final solution with AEP very close to that from the variable number program, being the solution of the former 0.50% lower than the latter, but requiring more WTs, and hence more investment (47% more). The final NPV value of the variable number model is 16.43% greater than the one with fixed 50 WTs. These figures could be expected to be similar even in situations where lower AEPs are obtained, if that compensates by augmenting overall financial metrics as the NPV.

530 This result shows the benefit of having optimization models that support variable number of WTs and accounting for metrics beyond AEP. The advantages may become even more pronounced for more complex situations, as for instance, if the WT investment costs are dependent on the exact installation area or different WT sizes are considered.

(a) AEP evolution.

(b) NPV evolution.

(c) Number of WTs evolution.
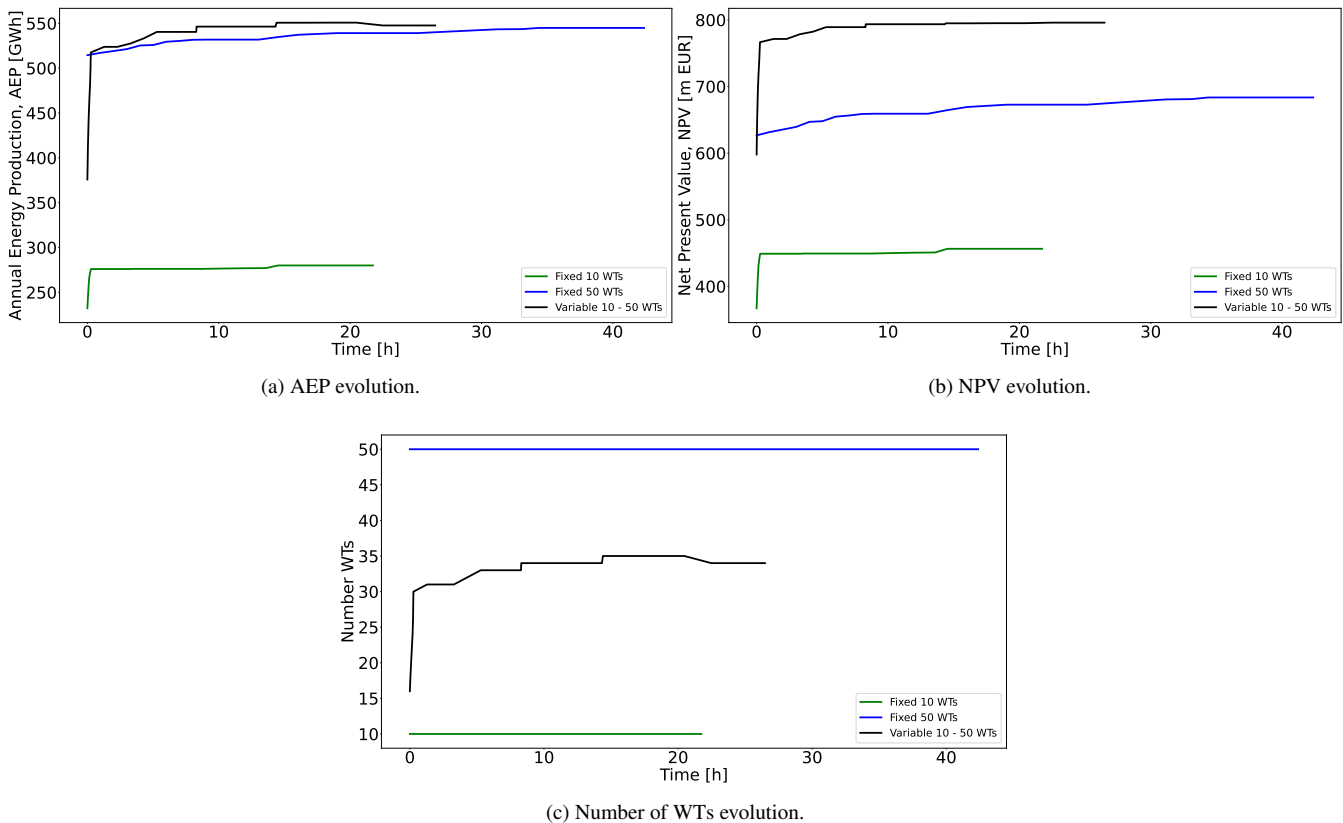
Figure 11. Evolution of the AEP, NPV, and number of WTs for the three simulations. The green lines are results for the optimization program with fixed number of WTs equal to 10, the blue ones equal to 50, and the black ones for the optimization program with variable number of WTs between 10 and 50.

27

6 Discussions

The two models proposed in this manuscript have many of the characteristics of mixed integer linear programming models. They require significant computational time and memory and exhibit rather low tractability and scalability for global optimization algorithms.

The power-curve-based model, albeit requiring large computational resources, manages to provide reasonably good solutions for small-sized problem, being only 1.18% lower than its power-curve-free counterpart for the 16 WTs case and 4.41% for the 36 WTs case. This diminishing efficiency is to be expected, given the large number of variables and constraints. The power-curve-free model on the other hand, along with the heuristic, is much faster due to its more compact formulation. This translates into the ability to be highly competitive compared to a large set of benchmark algorithms. In situations where there is an interest for optimizing metrics beyond AEP, such as the NPV, the power-curve-based model becomes very useful given its intrinsic capacity to support this kind of objective functions.

It should be mentioned that there are limitations in the wake models used compared to recent ones (Thomas et al., 2022b). For example, the wake model used in this manuscript does not consider the changes in the turbulence intensity or thrust coefficient variations from wind speed variations inside the wind farm. It is uncertain if using wake models like the ones in (Thomas et al., 2022b) would still allow an integer linear programming formulation or approximation of the WFLO problem. It is also uncertain the impact on the final solution quality these detailed modelling aspects imply. These questions are left for future work.

Notwithstanding the listed shortcomings, it is very enthralling that these models, in combination with the neighborhood search heuristic, are able to match and in some cases improve the results obtained when considering the turbine positions as continuous variables (see Table 3). This opens the door to experimenting case studies with functionalities easily adaptable to discrete parametrization techniques, which can be very challenging for continuous variable modelling approaches.

7 Conclusions

This manuscript contributes both methodologically and empirically to address the WFLO problem. A neighborhood search heuristic embedding integer programming formulations is proposed. For both presented formulations presented in the manuscript, the step-wise power curve and power-curve-free, the heuristic notably improves a single execution of full models when calling a state-of-the-art branch-and-cut solver in terms of solution quality. An improvement of up to 3.42% in the AEP is achieved by applying the neighborhood search strategy for cases where the WTs number is fixed compared to solving the full model.

Another important takeaway is the satisfactory performance of the power-curve-free model, which uses an approximation of the total wind speed deficit, when (implicitly) optimizing for AEP. This is due to the good correlation between the two measures, and the correction capability of the heuristic. For the classic WFLO problem definition, the proposed model is able to considerably improve (from 1% to around 10%) the AEP compared to benchmark results by multiple gradient-based and gradient-free algorithms. Even when directly compared to methods implementing a continuous variables technique, the proposed heuristic provides similar or even better results. These are very promising results that would enable to get high-quality

solutions for problem instances where continuous variables modelling approaches may not be able to run or provide with good incumbents.

Finally, the model with explicit representation of the power curve embedded within the neighborhood search heuristic is able to propose non-trivial solutions when implementing objective functions beyond AEP, such as NPV. For these cases, the trade-off between energy revenues and investment costs is inherently studied. For example, the model suggests that is installing a lower number of wind turbines than the allowed would results in a better NPV value, albeit a slightly lower AEP.

References

Archer, R., Nates, G., Donovan, S., and Waterer, H.: Wind turbine interference in a wind farm layout optimization mixed integer linear programming model, Wind Engineering, 35, 165–175, 2011.

Baker, N., Stanley, A., Thomas, J., Ning, A., and Dykes, K.: Best practices for wake model and optimization algorithm selection in wind farm layout optimization, in: AIAA Scitech 2019 Forum, p. 0540, https://doi.org/https://doi.org/10.2514/6.2019-0540, 2019.

Bastankhah, M. and Porté-Agel, F.: Experimental and theoretical study of wind turbine wakes in yawed conditions, Journal of Fluid Mechanics, 806, 506, https://doi.org/https://doi.org/10.1017/jfm.2016.595, 2016.

Cogency: A Refresher on Net Present Value, http://www.cogencygroup.ca/uploads/5/4/8/7/54873895/harvard_business_review-a_refresher_on_net_present_value_november_19_2014.pdf, 2014.

Fagerfjäll, P.: Optimizing wind farm layout-more bang for the buck using mixed integer linear programming (MSc. Thesis), Tech. rep., Chalmers University of Technology. Department of Mathematical Sciences, 2010.

Fischetti, M. and Lodi, A.: Local branching, Mathematical Programming, 98, 23–47, 2003.

Fischetti, M., Fischetti, M., and Monaci, M.: Optimal turbine allocation for offshore and onshore wind farms, in: Optimization in the real world, pp. 55–78, Springer, 2016.

Grady, S., Hussaini, M., and Abdullah, M.: Placement of wind turbines using genetic algorithms, Renewable Energy, 30, 259–270, https://doi.org/https://doi.org/10.1016/j.renene.2004.05.007, 2005.

GWEC: Global Wind Report 2019, Tech. rep., GWEC, https://gwec.net/global-wind-report-2019/, 2020a.

GWEC: Global Offshore Wind Report 2020, Tech. rep., GWEC, https://gwec.net/wp-content/uploads/2020/12/GWEC-Global-Offshore-Wind-Report-2020.pdf, 2020b.

Herbert-Acero, J., Probst, O., Réthoré, P.-E., Larsen, G., and Castillo-Villar, K.: A Review of Methodological Approaches for the Design and Optimization of Wind Farms, Energies, 7, 6930–7016, https://doi.org/10.3390/en7116930, 2014.

IBM: IBM ILOG CPLEX Optimization Studio CPLEX: User Manual, Tech. rep., IBM, https://www.ibm.com/docs/en/icos/12.10.0?topic=cplex, 2022.

IEA Wind Task 37, I. W.: Wake Model Description for Optimization Only Case Study, Tech. rep., International Energy Agency, https://github.com/byuflowlab/iea37-wflo-casestudies/blob/master/cs1-2/iea37-wakemodel.pdf, 2019.

Jensen, N.O.: A note on wind generator interaction, Report, Risø, Roskilde, Denmark, https://orbit.dtu.dk/files/55857682/ris_m_2411.pdf, 1983.

Katic, I., Højstrup, J., and Jensen, N.: A simple model for cluster efficiency, in: European Wind Energy Association conference and exhibition, vol. 1, pp. 407–410, 1986.

Kuo, J., Romero, D., Beck, J., and Amon, C.: Wind farm layout optimization on complex terrains–Integrating a CFD wake model with mixed-integer programming, Applied Energy, 178, 404–414, https://doi.org/https://doi.org/10.1016/j.apenergy.2016.06.085, 2016.

Lissaman, P.: Energy effectiveness of arbitrary arrays of wind turbines, Journal of Energy, 3, 323–328, https://doi.org/doi.org/10.2514/6.1979-114, 1979.

LoCascio, M. J., Bay, C. J., Bastankhah, M., Barter, G. E., Fleming, P. A., and Martínez-Tossas, L. A.: FLOW Estimation and Rose Superposition (FLOWERS): an integral approach to engineering wake models, Wind Energy Science, 7, 1137–1151, https://doi.org/10.5194/wes-7-1137-2022, 2022.

Mishnaevsky Jr, L. and Thomsen, K.: Costs of repair of wind turbine blades: Influence of technology aspects, Wind Energy, 23, 2247–2255, 2020.

Mittal, P. and Mitra, K.: Decomposition based multi-objective optimization to simultaneously determine the number and the optimum locations of wind turbines in a wind farm, IFAC-PapersOnLine, 50, 159–164, 2017.

620   Mosetti, G., Poloni, C., and Diviacco, D.: Optimization of wind turbine positioning in large wind farms by means of a genetic algorithm, Journal of Wind Engineering and Industrial Aerodynamics, 51, 105–116, https://doi.org/https://doi.org/10.1016/0167-6105(94)90080-9, 1994.

Niayifar, A. and Porté-Agel, F.: A new analytical model for wind farm power prediction, in: Journal of Physics: Conference Series, vol. 625, p. 012039, IOP Publishing, https://doi.org/10.1088/1742-6596/625/1/012039, 2015.

625   Nord Pool: Price Development, https://www.nordpoolgroup.com/en/, 2022.

Pearson, K.: VII. Note on regression and inheritance in the case of two parents, in: Proceedings of the Royal Society of London, vol. 58, pp. 240–242, The Royal Society London, https://doi.org/10.1098/rspl.1895.0041, 1895.

Pérez, B., Mínguez, R., and Guanche, R.: Offshore wind farm layout optimization using mathematical programming techniques, Renewable energy, 53, 389–399, 2013.

630   Pollini, N.: Topology optimization of wind farm layouts, Renewable Energy, 195, 1015–1027, https://doi.org/https://doi.org/10.1016/j.renene.2022.06.019, 2022.

Porté-Agel, F., Bastankhah, M., and Shamsoddin, S.: Wind-turbine and wind-farm flows: a review, Boundary-Layer Meteorology, 174, 1–59, 2020.

Quan, N. and Kim, H.: Greedy robust wind farm layout optimization with feasibility guarantee, Engineering Optimization, 51, 1152–1167, 635   2019.

Réthoré, P.-E., Fuglsang, P., Larsen, G., Buhl, T., Larsen, T., and Madsen, H.: TOPFARM: Multi-fidelity optimization of wind farms, Wind Energy, 17, 1797–1816, 2014.

Shaw, P.: Using constraint programming and local search methods to solve vehicle routing problems, in: International conference on principles and practice of constraint programming, pp. 417–431, Springer, 1998.

640   Stanley, A. and Ning, A.: Massive simplification of the wind farm layout optimization problem, Wind Energy Science, 4, 663–676, https://doi.org/https://doi.org/10.5194/wes-4-663-2019, 2019.

Thomas, J. and Ning, A.: A method for reducing multi-modality in the wind farm layout optimization problem, in: Journal of Physics: Conference Series, vol. 1037, p. 042012, https://doi.org/10.1088/1742-6596/1037/4/042012, 2018.

Thomas, J., Bay, C., Stanley, A., and Ning, A.: Gradient-Based Wind Farm Layout Optimization Results Compared with Large-Eddy Simu-
645   lations, Wind Energy Science Discussions, pp. 1–28, 2022a.

Thomas, J., McOmber, S., and Ning, A.: Wake expansion continuation: Multi-modality reduction in the wind farm layout optimization problem, Wind Energy, 25, 678–699, https://doi.org/10.1002/we.2692, 2022b.

Thomas, J. J., Baker, N. F., Malisani, P., Quaeghebeur, E., Perez-Moreno, S. S., Jasa, J., Bay, C., Tilli, F., Bieniek, D., Robinson, N., Stanley, A. P. J., Holt, W., and Ning, A.: A Comparison of Eight Optimization Methods Applied to a Wind Farm Layout Optimization Problem,
650   Wind Energy Science Discussions, 2022, 1–43, https://doi.org/10.5194/wes-2022-90, 2022c.

Turner, S., Romero, D., Zhang, P., Amon, C., and Chan, T.: A new mathematical programming approach to optimize wind farm layouts, Renewable Energy, 63, 674–680, 2014.

Voutsinas, S., Rados, K., and Zervos, A.: On the analysis of wake effects in wind parks, Wind Engineering, pp. 204–219, https://www.jstor.org/stable/43749429, 1990.

655 Wan, C., Wang, J., Yang, G., and Zhang, X.: Optimal micro-siting of wind farms by particle swarm optimization, in: International Conference in Swarm Intelligence, pp. 198–205, Springer, https://doi.org/https://doi.org/10.1007/978-3-642-13495-1_25, 2010.

Wolsey, L. A.: Integer programming, John Wiley & Sons, 2020.